

This work was written as part of one of the author's official duties as an Employee of the United States Government and is therefore a work of the United States Government. In accordance with 17 U.S.C. 105, no copyright protection is available for such works under U.S. Law. Access to this work was provided by the University of Maryland, Baltimore County (UMBC) ScholarWorks@UMBC digital repository on the Maryland Shared Open Access (MD-SOAR) platform.

Please provide feedback

Please support the ScholarWorks@UMBC repository by emailing scholarworks-group@umbc.edu and telling us what having access to this work means to you and why it's important to you. Thank you.

ACCEPTED MANUSCRIPT

The microglia response to electrical overstimulation of the retina imaged under a transparent stimulus electrode

To cite this article before publication: Alula R Yohannes *et al* 2021 *J. Neural Eng.* in press <https://doi.org/10.1088/1741-2552/abda0a>

Manuscript version: Accepted Manuscript

Accepted Manuscript is "the version of the article accepted for publication including all changes made as a result of the peer review process, and which may also include the addition to the article by IOP Publishing of a header, an article ID, a cover sheet and/or an 'Accepted Manuscript' watermark, but excluding any other editing, typesetting or other changes made by IOP Publishing and/or its licensors"

This Accepted Manuscript is © 2020 IOP Publishing Ltd.

During the embargo period (the 12 month period from the publication of the Version of Record of this article), the Accepted Manuscript is fully protected by copyright and cannot be reused or reposted elsewhere.

As the Version of Record of this article is going to be / has been published on a subscription basis, this Accepted Manuscript is available for reuse under a CC BY-NC-ND 3.0 licence after the 12 month embargo period.

After the embargo period, everyone is permitted to use copy and redistribute this article for non-commercial purposes only, provided that they adhere to all the terms of the licence <https://creativecommons.org/licences/by-nc-nd/3.0>

Although reasonable endeavours have been taken to obtain all necessary permissions from third parties to include their copyrighted content within this article, their full citation and copyright line may not be present in this Accepted Manuscript version. Before using any content from this article, please refer to the Version of Record on IOPscience once published for full citation and copyright details, as permissions will likely be required. All third party content is fully copyright protected, unless specifically stated otherwise in the figure caption in the Version of Record.

View the [article online](#) for updates and enhancements.

The microglia response to electrical overstimulation of the retina imaged under a transparent stimulus electrode.

Alula R. Yohannes¹, Christopher Y. Jung², Katherine I. Shea³, Wai T. Wong⁴, Alexander Beylin⁵, and Ethan D. Cohen¹

1. Division of Biomedical Physics
Office of Science and Engineering Labs
Center for Devices and Radiological Health
Food and Drug Administration
Bldg. 62 Rm 1204
White Oak Federal Research Labs
Silver Spring, MD 20993-0002
EMAIL: ethan.cohen@fda.hhs.gov
Tel (301) 796-2485
Fax (301) 796-9927

2. University of Maryland Baltimore County
1000 Hilltop Circle,
Baltimore, MD 21250
(410) 455-1000

3. Division of Applied Regulatory Science
Center for Drug Evaluation and Research
Food and Drug Administration
White Oak Federal Research Labs
Silver Spring, MD 20993-0002

4. National Eye Institute
Laboratory of Retinal Cell and Molecular Biology
6 Center Drive
National Institute of Health
Bethesda, MD 20814

5. Office of Health Technology 1
Office of Product Evaluation and Quality
Center for Devices and Radiological Health
Food and Drug Administration
Silver Spring, MD 20993-0002

Article Type: Paper.
Short Title Imaging microglia under transparent stimulus electrodes
MSWord
40 pages incl. 13 figures.

Abstract

Objective: We investigated using the morphological response of retinal microglia as indicators of tissue damage from electrical overstimulation by imaging them through an optically transparent stimulus electrode. *Approach:* To track the microglia, we used a transgenic mouse where the microglia expressed a water soluble green fluorescent protein (GFP). The clear stimulus electrode was placed epiretinally on the inner limiting membrane and the microglia layers were imaged using time-lapse confocal microscopy. We examined how the microglia responded both temporally and spatially to local overstimulation of the retinal tissue. Using confocal microscope vertical image stacks, the microglia under the electrode were imaged at 2.5min intervals. The retina was overstimulated for a 5 minute period using 1msec 749 μ C/cm²/ph biphasic current pulses and changes in the microglia morphology were followed for 1 hour post stimulation. After the imaging period, a label for cellular damage was applied to the retina. *Main results:* The microglia response to overstimulation depended on their spatial location relative to the electrode lumen and could result in 3 different morphological responses. Some microglia were severely injured and became a series of immotile ball-like fluorescent processes. Other microglia survived, and reacted rapidly to the injury by extending filopodia oriented toward the damage zone. This response was seen in inner retinal microglia outside the stimulus electrode edge. A third effect, seen with the deeper outer microglia under the electrode, was a fading of their fluorescent image which appeared to be due to optical scatter caused by overstimulation-induced retinal edema. *Significance:* The microglial morphological responses to electrical overstimulation injury occur rapidly and can show both direct and indirect effects of the stimulus electrode injury. The microglia injury pattern closely follows models of the electric field distribution under thinly insulated disc electrodes.

Introduction

In retinal prostheses, stimulus electrodes placed against the retinal surface generate current pulses which excite the local neurons. These pulses also cause currents to pass across neurons, glia, their processes, junctional barriers, and the interstitial fluid in the retina. When the charge density of these pulses is excessive this may cause injury to the retinal cells which can result in tissue swelling, retinal detachment, and the necrotic death of cells (ex. McCreery *et al.*, 1990). A variety of histopathologic methods have been used to study this neuronal damage to the retina, including upregulation of glial fibrillary acidic protein (GFAP) (Wen *et al.*, 1995), Fluoro Jade staining (Schmued and Hopkins, 2000), and classic hematoxylin-eosin staining (Colodetti, *et al.*, 2007). However, the histologic processing and evaluation of stimulated retinal tissue is time consuming and requires a pathologist for evaluating the tissue for injury. In addition, many histopathologic methods often require some cellular reaction time before processing the tissue for analysis (Ex. GFAP upregulation) which can distort the injury zone due to the phagocytosis of dead cells, tissue healing, and glial/retinal remodeling (ex. Wen *et al.* 1995, Lavinsky *et al.*, 2014).

Optical methods have also been used to study retinal tissue damage from electrical pulse overstimulation including using fluorescent DNA dyes to detect cellular damage (Butterwick, *et al.*, 2007, Cohen *et al.* 2011, O'Neill and Tung, 1991, McCreery *et al.*, 1990), and using optical coherence tomography (OCT) to study changes in retinal structure/scatter, (Cohen *et al.*, 2011). However, these methods often do not actually indicate that the neurons and glia in the retinal tissue are directly injured but are indirect. The disruption of the patency of the retinal membrane in the retina by damage due to electroporation can be detected by cellular incorporation of normally impermeant fluorescent nuclear dye DNA stains (ex. Butterwick *et al.*, 2007). However the pores allowing dye incorporation can be either reversible, or irreversible depending on the stimulus pulse duration (Benz and Conti, 1981). It is generally believed that detection of tissue damage is best examined when it is close to the time of the test insult (e.g.

1 Garman *et al* 2001, Nakauchi *et al* 2007, Bolon *et al* 2006). What is needed are the
2 development of sensitive markers of cellularly-relevant signals of injury that are intrinsic to the
3 retina that can rapidly detect the damage of the retinal tissue.
4
5
6
7

8 One injury-sensitive biomarker that is resident in retinal tissue are microglia. Microglia
9 form the major immune cell type present in the retina and central nervous system. In the
10 retina, these cells are thought to play key roles in immune surveillance, synaptic pruning,
11 regulation of neurogenesis and axonal growth, in addition to their role in the host's defense
12 system against cytotoxic or physical injury. Under normal conditions, the microglia are
13 uniformly distributed across the retinal surface as a series of layers of branched cells at several
14 retinal levels (ex. Vrabec 1970; Lee *et al.*, 2008). In their resting morphological state, they
15 exhibit a series of fine highly branched processes that are in constant motion probing the
16 extracellular space around the neurons and glia. When neural tissue becomes stressed,
17 microglial cells become activated; typically extending broad processes into the injury zone to
18 rapidly respond to acute insults such as focal laser burns, or penetrating electrodes (Eter *et al.*,
19 2008; Lee *et al.*, 2008; Nimmerjahn *et al.* 2005; Davalos *et al.*, 2005; Kozai *et al.*, 2012). In
20 addition, microglia are highly sensitive to cellular release of damage molecules such as ATP
21 which causes process extension (Davalos *et al.*, 2005).
22
23
24
25
26
27
28
29
30
31
32
33
34
35
36

37 Many epiretinal stimulus electrodes are opaque to light. This presents a problem as the
38 electric field is often strongest just below the opaque electrode but the underlying retina
39 cannot be visualized by current ophthalmic imaging techniques (ex. De Balthasar *et al.*, 2008).
40 We previously developed a method to examine retinal injury under stimulus electrodes by using
41 an optically transparent saline-filled FEP fluopolymer stimulation electrode tube (Cohen, 2009,
42 Cohen *et al.* 2011). Using this method, we were able to probe the retinal response under
43 stimulation electrodes by recording retinal network function from local ganglion cells, and
44 image the overstimulated retinal layers with OCT (Cohen, 2009, Cohen *et al.*, 2011). Here we
45 have combined real-time confocal microscopy under a transparent stimulus electrode to image
46 in real time the microglia morphological response to electrode overstimulation using a
47 transgenic mouse retina where the microglia are labeled with a green fluorescent protein (GFP).
48
49
50
51
52
53
54
55
56
57
58
59
60

Most previous retinal injury studies used lasers to ablate the retina tissue (and microglia) and the responses of only the surrounding surviving microglia were studied, so the morphologies of damaged microglia remaining in lesions are rarely described. We found the microglia response to electrode overstimulation was very rapid, and their morphological response to overstimulation injury could vary depending on whether the cells were directly injured by the overstimulation, or they responded to injury of the adjacent retinal tissue.

Methods

To track the microglia, we used the CX3CR1 EGFP (enhanced green fluorescent protein) homozygous strain of transgenic mice (Jackson Biologicals, Bar Harbor, Maine) where the microglia express a green fluorescent protein under control of the fractalkine promoter. These pigmented mice were crossed with a C57BL/6J mouse resulting in heterozygous progeny. Most of the experiments reported here (73X%) involved the use of these heterozygous mice for imaging purposes, although a few earlier experiments used homozygous mice similar to Eter *et al.* 2008. We did not observe large differences in the GFP fluorescence levels or kinetics between the heterozygous and homozygous pigmented CX3CR1 mouse microglia strains. The same low confocal 488nm laser power settings were used for imaging both strains. We imaged the microglia in the retina of mice aged 6 months to 1.3 years of age, due to the larger area of the retina.

Using a protocol approved by the White Oak FDA Institutional Animal Care and Use Committee (IACUC), a mouse was sacrificed using i.p. pentobarbital anesthesia (100mg/Kg) . The eyes were enucleated, hemisected, and the retinae were isolated. The isolated retinas were mounted on 13mm black nitrocellulose filter paper (Millipore HABP), and one filter was placed on the bottom of a custom made perfusion chamber for imaging. The isolated retina was perfused with a bicarbonate-based Ringer (Ames and Nesbett, 1981), (US Biologicals, Salem, MA) containing the following salts (mM) NaCl, 120; KCl, 3.1; KH₂PO₄, 0.5; NaHCO₃, 23.0; Mg₂SO₄, 1.2; CaCl₂, 1.15; 26 vitamins and amino acids, and equilibrated with carbogen. The second retina was held for future use in a gassed Ringer holding tank at room temperature. The Ringer flowed across the retinal tissue by gravity at a rate of 4-5 ml/min., and was heated by an in line heater to 34-35°C just before entering the retinal chamber. The temperature was monitored by

a thermocouple at the entrance to the chamber. The nuclear dye 7-amino actinomycin D (7AAD) (Cayman Chemicals, Ann Arbor, MI) was stored at 1 mg/ml in DMSO and kept frozen prior to use. A few earlier experiments used the nuclear dye propidium iodide with similar results.

Stimulation

A transparent tube FEP Teflon stimulation electrode was used to allow imaging the microglial response under the electrode to overstimulation (Fig.1) (See Cohen, 2009, Cohen *et al.*, 2011). To obtain an FEP transparent tube with adequate insulation thickness, we used FEP insulation wire sleeve (Type AS636 AWG32 Cooner Wire, Chatsworth CA) which had an inner diameter of ~210µm and a wall thickness of 65µm. A short ~4mm length of tube was faced flat at a 30 degree angle using a custom acrylic cutting jig, mounted on a pipette tip held in a syringe, and filled with Ames Ringer. The position of the tube was controlled visually using a Sutter MP285 micromanipulator mounted on the stage (Sutter Instruments, Novato CA). Careful alignment of the thinly insulated tube lumen edge (seen at high contrast in the first confocal image) to be flush to the retinal surface was critical for evoking effective stimulation damage with the small electrodes. A 3cm long 50µm diam Pt-Ir stimulus electrode wire was inserted into the syringe/tube and extended to within 1mm from the tip lumen to reduce access resistance. A 2cm long Pt-Ir wire (0.25mm diam) served as the counter electrode in the bath.

Using the Spike2 recording system, the computer controlled the stimulus isolator to produce cathodic-first 1msec biphasic stimulus current pulses, $749\mu\text{C}/\text{cm}^2/\text{ph}$, at 50Hz, which previous studies showed to induce retinal damage (Cohen *et al.*, 2011). We also examined in a few cases, lower levels of stimulation ($442\mu\text{C}/\text{cm}^2/\text{ph}$). The stimulus electrode charge densities were calculated based on the area of the electrode lumen. An AM3900 digital stimulus isolator (Everett Washington) controlled the polarity and timing of the pulses which were under computer control using a Micro II 1401 data acquisition unit and the Spike 2 programming language (Cambridge Electronic Design, Cambridge, UK). Stimulus current pulses from the isolator were capacitively coupled to the electrode whose DC voltage was monitored by a digital voltmeter. After each experiment the tube was carefully flushed and cleaned with alcohol and low retention detergent.

Imaging

A modified upright DMRE Leica TCS confocal laser microscope was used for time-lapse imaging the microglia under the stimulation electrode using a 20X 0.5NA water immersion objective. Preliminary experiments using 40X lenses could image only quadrants of the stimulation tube. To image the surrounding retina near the electrode, a series of 8-10 782µm x 782µm confocal Z-stacks were taken every 2.5min at 2Kx2K resolution. The image stacks were typically located 0.5-0.7mm eccentricity away from the optic disk. We used minimal 488nm laser power (8µW, Ophir Vega wattmeter) to excite the EGFP to avoid photobleaching, and the duty cycle of the intermittent scans was measured with a photodiode. This exposure was significantly below the ANSI Z80.36 group I safety limit of 440µW/cm². To verify stimulation damage was permanent and not due to transient electroporation, we applied the impermeant DNA stain 7AAD (1µg/ml) for 5 minutes to label the nuclei of dead cells at the end of the experiment. The confocal scan stacks were processed and registered into time lapse movies of the microglia for subsequent morphometric analysis using a series of custom ImageJ macros written using the FIJI image processing package (Schindelin *et al.*, (2012)). To study changes in scatter, summed image stack macros were used to avoid image saturation. Tracking of microglia cell bodies used soma-enhanced images and the TrackMate plug-in (Tinevez *et al.*, 2016). Only complete tracks during the imaging period were analyzed. The diameter of inner and outer microglia were derived from the summed and thresholded somal area from confocal substacks using the ImageJ particle analyzer function, and areas below 50µm² were excluded.

Results

We imaged the real time microglia response to retinal injury under an epiretinal stimulation electrode, by using a saline-filled transparent stimulation tube similar in conductive diameter to disk stimulus electrodes used in retinal prosthetic patients (Ahuja *et al.* 2013, Ayton *et al.*, 2014; Yue *et al.*, 2015, Cohen, 2009, Cohen *et al.*, 2011). Microglia are highly branched cells that are resident in the retina and are known to respond to retinal injuries such as laser burns with rapid changes in their resting morphology (Lee *et al.*, 2008, Eter *et al.* 2008). In order to study the microglia field around a stimulus electrode using a single microscope objective we chose a smaller stimulus electrode which allowed evaluation of the effects of electrical

1 stimulation on the microglia both inside and outside the tube at high spatial resolution. We
2 chose clear flat retinal regions for confocal imaging of overstimulation that were ~ 0.5-0.7mm
3 away from the optic disk and free of retinal blood vessels. In order to elicit a microglial
4 response to retinal injury with small electrodes with thin insulation, it was critical to obtain
5 close apposition and good effacement of the stimulus electrode lumen to the plane of the
6 retina (Majdi *et al.*, 2015). We used the first confocal image (contrast enhanced) of the
7 continuous edge of the electrode lumen as an alignment criteria for good effacement against a
8 planar field of microglia near the inner limiting membrane.
9
10
11
12
13
14
15
16

17 Time lapse movie construction

18 To comprehensively study the two layers of microglia under a stimulus electrode using time
19 lapse imaging, we needed to optically section through all the retinal microglia in the field in a
20 timely manner. Rapid image collection was performed by using large pinhole resonance
21 scanning confocal microscopy and image stacks of 8 or 10 sections. These vertical stacks
22 extended through the retina to average depth of $142.2 \pm 20.3\mu\text{m}$ (mean \pm s.dev.) from the
23 inner limiting membrane (n=9 experiments). Some padding was included for possible tissue
24 swelling. Time-lapse confocal images of the vertically sectioned stacks of the microglia during
25 the overstimulation experiment were projected for 2-D analysis using stack registration and
26 either the “summed” or “maximal intensity” Z-stack feature for image processing. To ensure
27 placement of the stimulation electrode tube had no effect on microglia number, we also
28 imaged unstimulated retinas under transparent tubes for over 75 minutes. While a few cells
29 showed slightly increased dendritic activity, we found there was little change in the position
30 of the majority of microglia and no change in their number under unstimulated electrodes,
31 and only minor changes were seen in the process arborization positions in the microglia field
32 around the electrode after 1 hour of imaging (n=3 retinas, see Movie 1, Fig.1 supplemental
33 data), similar to previous reports (See also Kozai *et al* 2012).
34
35
36
37
38
39
40
41
42
43
44
45
46
47
48
49
50

51 Figure 2 shows a confocal microscope image stack of the distribution of microglia in the
52 CX3CR1 mouse retina from a retinal slice. In the mouse, the microglia are distributed in 2
53 rough bands in the retina. In the inner retina, the microglia are positioned in a broad band
54
55
56
57
58
59
60

1 starting with superficial microglia near the inner limiting membrane surface and extending
2 through the inner plexiform layer. These microglia tended to be more heterogenous in their
3 morphology. A second more narrowly stratified band of microglia was located in the outer
4 plexiform layer (OPL). These outer cells appeared to exhibit more highly branched processes.
5 Using confocal microscope image analysis of the substacks of the two microglia layers from
6 the same Z-stack in the isolated retina, we measured the soma size distribution of 40 inner
7 and outer retinal microglia by analyzing 10 inner/outer cells from the same confocal stack in
8 4 different retinas (Figure 3). We found the soma diameters of inner retinal microglia were
9 larger and more variable, averaging $15.9 \pm 4.6\mu\text{m}$ (mean \pm std. dev), while the outer microglia
10 somas were smaller and more narrowly distributed averaging $10.3 \pm 1.6\mu\text{m}$ (mean \pm std. dev).
11 This difference was highly significant ($p < .00001$, unpaired T-test 2 indep. means).
12
13
14
15
16
17
18
19
20
21
22
23
24
25
26
27

28 We analyzed the microglial morphological responses to retinal overstimulation under a
29 transparent electrode using a series of zones and time-lapse confocal microscopy (Figure 4). To
30 ensure an injurious response to the retina, we stimulated the retina for 5 minutes with 50Hz
31 biphasic pulse trains at a charge density of $749\mu\text{C}/\text{cm}^2/\text{ph}$, which previous studies found to
32 generate significant retinal swelling (Cohen *et al.*, 2011). Multiphysics models of the electric
33 field of thinly insulated disc stimulus electrodes placed near a resistive surface/retinal tissue
34 indicate the E-field is strongest near the conductor's edge (ex. Wiley and Webster, 1982;
35 Minnikanti *et al.*, 2010). We were able to locate the position of the transparent stimulation
36 tube edges on the retinal surface by examining enhanced contrast confocal images of the first
37 scan in the stack. The cellular damage under the stimulation electrode was analyzed by cell
38 counts in three concentric elliptical zones. The first analysis zone was the outer width of the
39 electrode insulation of $65\mu\text{m}$ (wall), while the second inner analysis zone included inner
40 conductive lumen's edge to $65\mu\text{m}$ inside the lumen, while the third analysis zone included the
41 remaining area of the central (inner) lumen. For comparison, a small unstimulated triangular
42 zone ($29,800\mu\text{m}^2$) in the corner of the image away from the electrode was chosen as a control
43 for each experiment.
44
45
46
47
48
49
50
51
52
53
54
55
56
57
58
59
60

Effect of overstimulation on the retinal microglia under the stimulus electrode.

The effects of overstimulation on the microglia population under the stimulus electrode is shown by confocal microscope summed Z-stacks of the retina before ($t=7.5\text{min}$) and after ($t=67.5\text{ min}$) the stimulation period in Figure 5 and Movie 2. The first 4 images show confocal Z-stacks of the microglial distribution in the unstimulated control condition. The microglia are distributed in a rough pattern that covers the retinal surface, with the position of the electrode lumen over the surface shown as a dotted line. Other than slight movements of the processes, there is no change in the number of microglia. At the 10 minute point, the electrical pulse train stimulation started and a slight retraction of processes by the microglia inside the lumen of the electrode was seen which became more pronounced 2.5 min later. Then, the images of a microglia group with small somas in the electrode lumen began to fade. By the end of the 5 min of stimulation period, the filopodia of the microglia outside the electrode wall began to respond to the injury by extending filopodia non-directionally. Ten minutes after stimulation, the majority of microglia inside the electrode lumen became a series of ball-like connected strands exhibiting little or no process movement suggesting they were severely injured. The filopodia of the surviving microglia outside the electrode wall began to orient toward the electrode lumen and extended processes inwards. A dark gap of missing fluorescent processes of microglia began to develop across the retina in an elliptical ring under the electrode wall. Fifty minutes after stimulation, the microglia around the electrode wall continued extending filopodia into the electrode zone, with the microglia down from the electrode in the flow of Ringer (lower left) extending more processes than those “upwind” of it (upper right). The filopodia of microglia located in the periphery of the imaging field showed only small effects from the electrical overstimulation, and their processes in aggregate did not show a consistent bias of orientation.

To study the rapidity of the change in the microglia processes before and after stimulation, we superimposed the images of the microglia field taken just before overstimulation to 2.5, 12.5, 22.5, and 32.5 minutes post stimulation ($n=5$ retinas). Figure 6 shows the microglia field from the same retina above at the start of the imaging series ($t=0$), 2.5 minutes after stimulation and 12.5 minutes after stimulation. In each panel the microglial field

just prior to stimulation is colored red ($t=7.5\text{min}$), while the comparison field at the different time point is shown superimposed in green. Comparison of the unstimulated microglia at the start of the imaging session and at 7.5 minutes showed only minor changes in processes morphology causing the overlapped images to appear yellow. In contrast, 2.5 minutes after overstimulation, many microglia changed their morphology with green process growth (arrowheads) toward the electrode wall, while a few microglia in the far periphery remain unchanged. By 12.5 minutes post stimulation, many microglia around the electrode grew oriented green processes toward the damage zone. The few cells that remain unchanged appear yellow. A similar rapid temporal onset of process growth during overstimulation was seen on all the retinas examined.

Overstimulation had three different effects on the retinal microglia morphology

Overstimulation had three different effects on the retinal microglial morphology around the stimulus electrode. The first morphological response after the electrical stimulation period was a microglia with motile filopodia in the control condition, that became highly blebbed and immotile after the stimulation pulses (Figure 7A). After stimulation, these “immotile microglia” became a series of connected highly fluorescent ball-like membranes. These structures remained non-moving for the remainder of the imaging period suggesting they had sustained irreversible injury from the stimulation. The “immotile” response was the most common post stimulation morphology observed for microglia located in the electrode electrode lumen and wall zone.

A second set of cells, which we termed “responder” microglia appeared to survive the stimulation pulse period (Figure 7B). These cells resembled previous descriptions of “activated” microglia responding to laser injury (Lee *et al.*, 2008, Davalos *et al.*, 2005, Nimmerjahn *et al.*, 2005). During the unstimulated control period, they were extending and retracting small fine filopodia in a non-selective manner similar to resting microglia. Near the end of the 5 min. pulsing period, responder microglia initially reacted to the injury by exhibiting transient non-oriented filopodia efflorescences. After the pulsing period, the responder microglia retracted many of their filopodia, and they changed the orientation of their processes from the control condition by extending long filopodia oriented towards the zone of overstimulation injury. Near the electrode, these “responders” typically extended processes over or against the electrode

1 wall. Many responder microglia” could also be seen extending oriented filopodia all around the
2 periphery of the transparent tube post stimulation, with the more numerous filopodia
3 extensions always occurring on the lower left side of the tube “downwind” of the flow of Ringer
4 across the retinal surface (See Discussion). The few microglia inside the electrode lumen
5 survived pulsing, became “responders”. These surviving cells retained a distinct cell body post
6 stimulation and exhibited rapid kinetic movements of their extended filopodia in all directions
7 inside the lumen.
8
9
10
11
12
13
14

15 A third subset of the microglia had images that appeared to disappear/fade after the electrical
16 overstimulation which we termed “fading microglia” (Figure 7C). These fading microglial cells
17 had smaller cell bodies, and appeared to have finely branched dendritic arborizations. Fading
18 microglial cells were most often seen under the lumen and edges of the transparent electrode.
19 Unlike the injured fluorescent immotile inner microglia in the lumen during the confocal laser
20 scan, the soma of these cells were dimly detectable under the electrode as their images
21 appeared present in an increased background of fluorescent optical scatter. It was difficult to
22 ascertain from the scatter in the images if this class of microglial cells under the electrode were
23 in fact injured post-stimulation.
24
25
26
27
28
29
30
31
32

33 **Determining the identity of the fading microglia in the retina.**

34 Conceivably, the “fading” of a microglia could occur after overstimulation for 2 possible
35 reasons in confocal imaging. It is possible the microglia cells’ membranes were so disrupted
36 into vacuoles after the pulsing that there was little soluble GFP protein in the intact cell. This
37 phenomena occasionally appeared to occur to larger microglia post stimulation under the
38 electrode walls. Alternatively, we noted that groups of small soma microglia inside the
39 lumen appeared to simultaneously fade during the overstimulation images. We noted
40 microglia with small soma diameters were mainly found in the microglia branching in the
41 outer plexiform layer (ex. Fig 3). To examine this possibility, we developed movies of a field
42 of outer microglia during pulsing using only the substack of outer retinal layer stack images
43 An image of the outer microglia field inside the stimulus electrode lumen before pulsing is
44 seen in Figure 8A. Immediately after the overstimulation pulse trains, all the outer microglia
45 in the field in the lumen faded, suggesting these OPL microglia accounted for the “fading”
46
47
48
49
50
51
52
53
54
55
56
57
58
59
60

morphological response type observed in the time lapse image stacks (Figure 8B). In contrast, outside the electrode wall, the OPL microglia remained visible. A similar fading field pattern was seen in all cases (7/7) where we were able to image the outer microglia in the electrode lumen.

Overstimulation appears to cause edema under the electrode lumen

What mechanism was causing the outer GFP-labeled microglia to disappear in the confocal image during pulsing was unclear. However we noted three lines of evidence suggesting that retinal swelling under the electrode lumen during the stimulation pulses could account for this screening phenomena. First, time-lapse z-stack movies of the “fading” cells in the lumen during overstimulation showed that an increased optical scatter “background” was causing a loss of the normally transparent inner retinal layers above the OPL microglia and this produced more scatter of the fluorescence in the images, similar to our previous results using transparent electrodes at these charge densities and OCT imaging (Cohen *et al.*, 2011). Figure 8C shows a time lapse images of the ratio of the fluorescent scatter of a 50x50um ROI (region of interest) in the electrode lumen compared to an equivalent ROI region in the imaging field periphery. After excessive stimulation, the ratio of fluorescent confocal scatter signal in the electrode lumen to the periphery increased rapidly. In the control unstimulated condition, we found using 4 image stack averages, the scatter ratio of the tissue averaged 1.2 ± 0.07 AU (arbitrary units) (0-7.5min), while 4 stacks taken 2.5 min after stimulation averaged 2.0 ± 0.19 AU (n=8 retinas, mean \pm s.dev.) a 56% increase, which suggested significant tissue scatter in the electrode lumen was present after overstimulation. In 3 cases where we performed histology of the stimulated retinas at the end of the experiment, we found large fields of the inner retina were edematous. Fig 8.D shows a histological section of retina from an overstimulated zone next to a normal area, showing the swelling in the IPL. Furthermore, tracking experiments on fields of outer retinal microglia somas around the electrode from the movies of overstimulation (these cells were not fixed by the touching of the stimulus electrode to the inner limiting membrane) showed that the OPL microglia somas outside the electrode were rapidly displaced centrifugally post

stimulation relative to the electrode center an average of $37.2 \pm 12.5 \mu\text{m}$ $n=6$ retinas (mean 6 cells/retina, std dev) (Figure 8E). These rapid displacements of whole fields of microglia were clearly due to large displacements of the retinal tissue and not migrations of the microglia cell bodies themselves. The results of these experiments all provided evidence that overstimulation caused a rapid edema in the neuropil under the electrode that declined only partially over an hour of imaging the retina post stimulation.

The timcourse of microglia injury under the stimulus electrode after overstimulation.

We analyzed how microglia were injured by overstimulation in different zones around the electrode lumen by analyzing the larger inner retinal microglia under the stimulus electrode. The small microglia in the outer retina were not analyzed as their processes faded making analysis difficult. Microglia stimulation outcomes were scored based on their initial cell body prestimulus position ($t=7.5$ min.). Cell bodies covering two regions of interest were further measured to determine which zone occupied $> 50\%$ of the cell body which became their starting position. Figure 9 shows a summary diagram of the timecourse of microglial injury after overstimulation. Using confocal scan summed z-stacks, we analyzed the microglia morphological outcomes after overstimulation using the 3 concentric elliptical zones under the stimulus electrode. These zones were: the wall zone- known to have a strong electromagnetic field during stimulus pulses, the inner edge zone, and the central lumen of the electrode (Wiley and Webster, 1982, Minnikanti *et al.*, 2010). The width of the outer 2 evaluation zone bands were the thickness of the electrode wall ($65\mu\text{m}$). The number of live microglia were counted pre stimulation (0, 7.5 min), and 2.5, 12.5 min or 52.5 minutes post pulse stimulation (67.5 min.). For the 4 prestimulus frames there were no changes in the number of microglia observed, and only small changes were seen in the movements of their filopodia (See also Movie 2 for a field example, and cell samples Movies 3-5). Microglia were classified as either live or dead. Dead microglia included ball-like "immotile" cells and the few cells that lost their fluorescence into particles near the electrode wall. After overstimulation the number of live microglia rapidly declined at the first analysis point 2.5 min post stimulation. The losses of the average number microglia in each of the 3 zones were highly significant, and the loss continued to the end of the analysis period 52.5 minutes

1 post stimulation. However there were not significant differences in the rate of death for
2 cells between the electrode walls, inner edge , and in the inner lumen zones. It may be that
3 microglia process orientation to the wall plays a role in cell survival. It also was not clear what
4 were the identity of the microglia reacting to overstimulation in the different retinal layers.
5
6
7
8
9
10
11
12
13
14

15 **Determining which microglia layers responded and were injured by overstimulation under**
16 **the electrode.**
17

18 To the identity the microglia layers reacting to overstimulation injury we used a depth color
19 coding scheme for the microglia layers. Time-lapse confocal images of the vertical sectioned
20 stacks of the microglia during the overstimulation experiment were depth color coded by their
21 confocal Z-section imaging position in the retina using a color look up table macro (Figure 10,
22 and Movie 6). The inner microglia tended to be colored yellow to blue, while the distal
23 microglia in the outer plexiform layer were colored red or pink. We found after the electrical
24 overstimulation period that many inner retinal microglia in the lumen (yellow-cyan) were
25 disfigured into ball-like membranes and immotile. These inner microglia were almost always
26 the microglia closest to the stimulus electrode tube face. The fates of the outer microglia after
27 overstimulation were more difficult to assess due to image fading due to scatter, but we noted
28 in 4/5 cases their somas appeared to survive the stimulation period intact. Outside of the
29 electrode wall, the inner retinal microglia were identified as the “responder” cell morphologies
30 extending filopodia across and against the electrode wall. In contrast while the outer microglia
31 just outside the electrode wall (pink) could display a transient filopodia extension responder
32 morphology during the stimulation period, this rarely resulted in extended filopodia growth
33 towards the lumen zone when time lapse imaged for over 1 Hr (see Movie 6).
34
35
36
37
38
39
40
41
42
43
44
45
46
47

48 Figure 11 shows a dot plot summary data identifying the retinal depth location of any
49 responder microglia outside the electrode lumen showing filopodia growth oriented towards
50 the tube at the 67.5 min timepoint (52.5 min post stimulation). Responding microglia were
51 tracked back to their position pre-stimulation (t=7.5min) to identify their soma position in the
52 mouse’s retinal layers. Each microglia’s initial position is shown by a single black dot. Microglia
53
54
55
56
57
58
59
60

soma depth position results are shown from 4 experiments, from a total of 43 microglial cells, with 0 being the top of the inner limiting membrane (ILM). On average $89.4 \pm 9.5\%$ (n=4 expts, mean, Std. Dev.) of the “responder” microglia originated from the inner retina, usually within 50um of the surface of the ILM, as these microglia are closest to the stimulation electrode on the surface of the ILM. Analysis of movement of microglia somas indicated there was little upward movement of most microglia somas after overstimulation, averaging less than one confocal vertical scan step (mean= 0.47 focus steps, n=4 expts).

Lower charge density stimulation.

We also examined the effects of 442uC/cm²/ph stimulation on a limited sample of 3 retinas. Fig. 12 shows a montage of 2 microglia in the electrode lumen at 4 time points during the 442uC/cm²/ph overstimulation. At this charge density, there was less damage to the microglia inside the electrode lumen in 2/3 cases. Again, during overstimulation, the outer retina microglia images disappeared. The inner microglia often grew processes rapidly during the end of stimulation, which were then retracted upon recovery. It appeared there was less process extension from microglia outside the lumen into the lumen (responder cells).

7AAD staining of the retina in the post-stimulation period.

The nuclear dyes propidium iodide and 7AAD have been used to label dead cells in retinas where the membranes of cells have been comprised due to injury, allowing the nucleus become fluorescent by binding to the chromatin. The ability of the 7AAD dye to brightly stain dead cell nuclei was confirmed by imaging tiny retinal cuts, acutely labeled with 7AAD (n=2) (unpublished observations). After an imaging period of 60 minutes post stimulation, 7AAD was bath applied to the retina for 5 minutes, followed by a >5 min wash period (n=9 retinas). A denser series of confocal Z-stacks steps (typically 25 sections) were used to image deeply into the stimulation zone. We found 7AAD stained a series of small round nuclei in the inner retina just underneath the electrode edge and also around the outside of the stimulation zone (Figure 13). As noted previously (Bernier *et al.*, 2012, Innocenti *et al.*, 2004), the nuclei of activated microglia and also Muller cell endfeet were often labeled by nuclear dyes (Uckermann *et al.*, 2004). Under the electrode wall, some round nuclei appeared to be labeled by 7AAD.

However, inside the lumen the immotile microglia showed moderate stain, particularly in cases

where there was severe damage to the lumen microglia causing tissue scatter and edema. At 442uC/cm2/ph there appeared to be more extensive 7AAD labeling of the nuclei in the lumen tissue and at electrode edge (n=3 retinas) (Fig 13B). This could indicate severe cellular edema by 749uC/cm2/ph pulsing may cause more optical scatter causing reduced 7AAD fluorescence. It is also possible the overstimulation could disrupt nuclear dye binding sites on histone proteins with the DNA (ex. Banerjee *et al.*, 2014).

Discussion

We have developed a method to study retinal injury in real time under by using an optically transparent saline-filled stimulus electrode tube similar in form factor to electrodes used in retinal prostheses (Yue *et al*, 2015, Ahuja *et al.*, 2013). Combining this method with confocal microscopy in a transgenic mouse with labeled microglia, we have been able to real-time image the morphological response of an immune cell sensitive to retinal injury directly under a disk stimulus electrode during the delivery of excessive stimulus current pulses to the retina. Our real-time transparent tube imaging method allows a fuller understanding of the microglial temporal reaction to excessive charge density pulses causing injury under an electrode by allowing continuous imaging before, during and after the stimulation period. Unlike the studies of retinal injury produced by spots of lasers, we were also able to directly identify injured microglia morphologies to electrical stimulation in a quasi- three dimensional manner around the stimulus electrode. This allowed us to gain a better understanding of how all the microglia layers of the retina reacted spatially to excessive electrical stimulation pulses delivered by electrodes at the inner retinal surface.

We found that the changes in the microglial morphology in response to retinal injury during overstimulation was very rapid, in some cases occurring during the first 2.5 minute imaging frame. In most cells just outside the stimulus electrode, the initial response to overstimulation was a transient retraction of cytoplasm (See also Davalos *et al.*, 2005), followed by a burst of filopodia, whose processes rapidly oriented towards the injury zone if the microglia survived the injury and became a “responder” morphology. This is similar to reports of microglia using lasers to injure retinal and brain tissue (Davalos *et al*, 2005, Nimmerjahn *et al.*, 2005; Eter *et al.*, 2008; Lee *et al.*, 2008,). Over our imaging time of an hour, the filopodia of “responder”

1 microglia oriented and grew into the zone of injury often traversing under the electrode wall.
2 The bath Ringer flows around the stimulation tube/ injury zone. The number of “responder”
3 microglia filopodia behind the stimulation tube was always larger than filopodia number in
4 oriented microglia in front of the tube. This suggests that overstimulation of the retina
5 underlying the electrode may cause the release of soluble cytokine-like factors from injured
6 cells which are higher in the zone of less exchange. One known factor released by cellular injury
7 is the chemokine ATP, as release of ATP (or adenosine) by injured tissue is well known for
8 evoking filopodia extensions in microglia (Devalos, *et al.*, 2005, Fontainhas *et al.*, 2011). Both
9 cell stretch from edema and electroporation can also cause ATP release from neurons and glia,
10 (Hamann and Attwell, 1996; Xia *et al.* 2012; Newman, 2001).
11
12
13
14
15
16
17
18
19
20
21
22
23

24 While electrical overstimulation produced visible injury to the fluorescent microglia in
25 the inner retina, it is likely the surrounding retinal tissue was also injured by these electrical
26 current pulses. Three of our experimental results provide evidence the retinal tissue under the
27 stimulation tube was also injured. These findings are shown in a model (Figure 14). First, using
28 confocal fluorescent signal analysis of stimulated zones of retina, there was an increase in
29 fluorescent emission scatter present in the summed intensity full z-stacks of the retina neuropil
30 under the stimulated lumen, relative to stacks from unstimulated zones in the image periphery,
31 and that the time course of the scatter increase always coincided with onset of the stimulus
32 pulse trains. Secondly, during the imaging of the microglia, the microglia cell bodies
33 surrounding the stimulation electrode appeared to expand away from under the electrode wall
34 during the pulse stimulation period, particularly the outer microglia retina which were not fixed
35 by touching the electrode. Most of this displacement occurred during the stimulus pulse train
36 or shortly afterwards. This is consistent with overstimulation causing some form of tissue
37 edema expanding the retinal tissue under the electrode. Finally, histological analysis of
38 stimulated zones after the imaging session showed large edematous zones in the inner
39 plexiform layer and the inner part of the inner nuclear layer which would account for the
40 scattering loss of the fluorescent signal of the outer retinal microglia in the confocal microscope
41 when imaged through the inner retinal layers (see also Griffiths, *et al.*, 1986, McLaren *et al.*,
42
43
44
45
46
47
48
49
50
51
52
53
54
55
56
57
58
59
60

1
2
3
4
5
6
7
8
9
10
11
12
13
14
15
16
17
18
19
20
21
22
23
24
25
26
27
28
29
30
31
32
33
34
35
36
37
38
39
40
41
42
43
44
45
46
47
48
49
50
51
52
53
54
55
56
57
58
59
60

2010). The time course of the increases in retinal swelling would be consistent with our previous OCT studies with a larger transparent stimulus electrode in the rabbit retina. Cross sectional scans showed a rapid increase in the reflectivity (scatter) and swelling of the edematous inner retina during stimulation (Cohen *et al.* 2011). In retinal prostheses, disc stimulation electrodes are often mounted in an insulating array of polymer, and placed near the retinal surface. Our results imply if overstimulation causes swelling under an electrode, it is likely the tissue will move laterally due to confinement by the polymer tube material.

The outer microglia appear to respond to pulse train injury of the inner limiting membrane, with some process extension, however their response to the epiretinal electrode overstimulation appears to be smaller (ex. Figure 9). This may be due to the electric field declining with distance from the lumen at the inner retinal surface, diffusion of injury factors that cause microglial activation having farther to diffuse into the outer retinal tissue, and their smaller somal cross section could make them more resistant to direct electroporative current injury (Grosse and Schwan, 1992; Agarwal *et al.*, 2007). While the overstimulated tissue under the lumen appeared to be constrained from expanding vertically due to the overlying electrode and the underlying filter, this may have caused an outward expansion of the swollen retina which we measured as a centrifugal displacement in the outer microglia. These same cells appeared to compose the fading microglia image population due to scatter under the electrode. Future research will be needed to determine if these outer microglia under the electrode are injured post-stimulation.

Microglia cells at the ILM and in the IPL were located close to epiretinal electrode lumen at the retinal surface, and they responded rapidly to the overstimulation. This shows if it is possible to label these cells in patients with ICG similar to the rodent retina, they would provide good clinical indicators of safe stimulation levels for epiretinal electrode arrays (Paques *et al.*, 2010, Sim *et al.*, 2015). However it is unclear if these same microglia layers will respond as quickly to damage caused by subretinal and suprachoroidal electrode designs (Ayton *et al.*, 2014, Nakauchi *et al.*, 2007). Dendritic and macrophage immune cells are also involved in immune surveillance for implants with electrodes located in the choroid. However it is unclear which immune cell will be the responder to subretinal or suprachoroidal electrode overstimulation

and how quickly the damage will be detected. In some retinal degenerative diseases, macrophages may invade across the choriocapillaris into the subretinal space. The outer plexiform layer microglia are also located closer to the subretinal space in the degenerate retina, so future studies will be need to understand how the body's immune cells respond to overstimulation damage in these zones in the blind prosthetic patient.

We have developed a method to image neural immune cells called microglia that respond to tissue injury directly below a transparent disc stimulus electrode. The vast majority of neurostimulation devices used clinically rely on electrical stimulation for activation of the neural tissue using disc- or band-shaped electrodes. While microglia are found in the central nervous system, their dendritic cell counterparts are present on epithelia throughout the body. Our imaging technique may have clinical utility for evaluating safe stimulation levels of neurostimulatory devices in a variety of different body locations.

Acknowledgements: We thank Randall Bidinger and Fred Jordan for help in device fabrication, Anant Agrawal for technical assistance, Cooner Wire Co., Chatsworth CA for FEP wire samples, Joseph Madji for early experiments, and Peter Pecoraro (Leica Microsystems), Woody Strzelecki, Bennet Walker, Paul Yates (U Va Med School) and Owen Schwartz (NIAID/NIH microscopy) for assistance with rebuilding of the upright confocal microscope.

Disclaimer: The mention of commercial products, their sources, or their use in connection with material reported herein is not to be construed as either an actual or implied endorsement of such products by the Department of Health and Human Services.

References

Agarwal A, Zudans I, Weber EA, Olofsson J, Orwar O, Weber SG. 2007 Effect of cell size and shape on single-cell electroporation. *Anal Chem.* **79** 3589-96. PubMed PMID 17444611

Ahuja AK, Yeoh J, Dorn JD, Caspi A, Wuyyuru V, McMahon MJ, Humayun MS, Greenberg RJ, Dacruz L. 2013 Factors Affecting Perceptual Threshold in Argus II Retinal Prosthesis Subjects. *Transl Vis Sci Technol.* **2** 1 PubMed PMID 24049718

Ayton LN, Blamey PJ, Guymer RH, Luu CD, Nayagam DA, Sinclair NC, Shivdasani MN, Yeoh J, McCombe MF, Briggs RJ, Opie NL, Villalobos J, Dimitrov PN, Varsamidis M, Petoe MA, McCarthy CD, Walker JG, Barnes N, Burkitt AN, Williams CE, Shepherd RK, Allen PJ; Bionic Vision Australia Research Consortium. 2014 First-in-human trial of a novel suprachoroidal retinal prosthesis. *PLoS One.* **9** e115239. PMID 25521292

Banerjee A, Majumder P, Sanyal S, Singh J, Jana K, Das C, Dasgupta D. 2014 The DNA intercalators ethidium bromide and propidium iodide also bind to core histones. *FEBS Open Bio.* **4** 251-9. PubMed PMID 24649406

Bernier LP, Ase AR, Boué-Grabot E, Séguéla P. 2012 P2X4 receptor channels form large noncytolytic pores in resting and activated microglia. *Glia.* **60** 728-37. PubMed PMID 22318986.

Benz R, Conti F. 1981 Reversible electrical breakdown of squid giant axon membrane. *Biochim Biophys Acta.* **645** 115-23. PubMed PMID 6266473

Bolon B, Garman R, Jensen K, Krinke G and Stuart B (Ad Hoc Working Group of the STP Scientific and Regulatory Policy Committee) 2006 A 'best practices' approach to neuropathologic assessment in developmental neurotoxicity testing—for today. *Toxicol. Pathol.* **34** 296–313.

Butterwick A, Vankov A, Huie P, Freyvert Y and Palanker D 2007 Tissue damage by pulsed electrical stimulation *IEEE Trans. Biomed. Eng.* **54** 2261–7

Cohen ED. 2009 Effects of high-level pulse train stimulation on retinal function. *J Neural Eng.* **6** 035005. PubMed PMID 19458404.

1 Cohen E, Agrawal A, Connors M, Hansen B, Charkhkar H, Pfefer J. 2011 Optical coherence
2 tomography imaging of retinal damage in real time under a stimulus electrode. *J Neural Eng.* **8**
3 056017 PubMed PMID 21934187.

4
5
6
7 Colodetti L, Weiland J D, Colodetti S, Ray A, Seiler M J, Hinton DR and Humayun M S 2007
8 Pathology of damaging electrical stimulation in the retina *Exp. Eye Res.* **85** 23–33
9

10
11
12
13
14
15 Davalos D, Grutzendler J, Yang G, Kim JV, Zuo Y, Jung S, Littman DR, Dustin ML, Gan WB. 2005
16 ATP mediates rapid microglial response to local brain injury in vivo. *Nat Neurosci.* **8** 752-8.
17 PubMed PMID 15895084
18

19
20
21
22 de Balthasar C, Patel S, Roy A, Freda R, Greenwald S, Horsager A, Mahadevappa M, Yanai D,
23 McMahon MJ, Humayun MS, Greenberg RJ, Weiland JD, Fine I. 2008 Factors affecting
24 perceptual thresholds in epiretinal prostheses. *Invest Ophthalmol Vis Sci.* **49** 2303-14. PubMed
25 PMID 18515576
26
27
28

29
30
31 Eter N, Engel D R, Meyer L, Helb H M, Roth F, Maurer J, Holz F and Kurts C 2008 In vivo
32 visualization of dendritic cells, macrophages, and microglial cells responding to laser-induced
33 damage in the fundus of the eye. *Invest. Ophthalmol. Vis. Sci.* **49** 3649–58
34
35
36

37
38 Fontainhas A, Wang M, Liang KJ, Chen S, Mettu P, Damani M, Fariss R, Li W, Wong W. 2011
39 Microglial morphology and dynamic behavior is regulated by ionotropic glutamatergic and
40 GABAergic neurotransmission. *PLoS One.* Jan 25;6(1):e15973.
41 doi:10.1371/journal.pone.0015973 PMID: 21283568
42
43
44

45
46
47
48 Garman R H, Fix A S, Jortner B S, Jensen K F, Hardisty J F, Claudio L and Ferenc S 2001 Methods
49 to identify and characterize developmental neurotoxicity for human health risk assessment. II:
50 Neuropathology. *Environ Health Perspect.* 109 Suppl 1 93–100 PMID: 11250809
51
52
53
54
55
56
57
58
59
60

1
2
3
4
5
6
7
8
9
10
11
12
13
14
15
16
17
18
19
20
21
22
23
24
25
26
27
28
29
30
31
32
33
34
35
36
37
38
39
40
41
42
43
44
45
46
47
48
49
50
51
52
53
54
55
56
57
58
59
60

Griffiths SN, Drasdo N, Barnes DA, Sabell AG. 1986 Effect of epithelial and stromal edema on the light scattering properties of the cornea. *Am J Optom Physiol Opt.* **63** 888-94. PubMed PMID 3789079.

Grosse C, Schwan HP. 1992 Cellular membrane potentials induced by alternating fields. *Biophys J.* **63** 1632-42. PubMed PMID 19431866

Hamann M, Attwell D. 1996 Non-synaptic release of ATP by electrical stimulation in slices of rat hippocampus, cerebellum and habenula. *Eur J Neurosci.* **8** 1510-5. PubMed PMID 8758958.

Innocenti B, Pfeiffer S, Zrenner E, Kohler K, Guenther E. 2004 ATP-induced non-neuronal cell permeabilization in the rat inner retina. *J Neurosci.* **24** 8577-83. PubMed PMID 15456831

Kozai TD, Vazquez AL, Weaver CL, Kim SG, Cui TJ 2012 In vivo two-photon microscopy reveals immediate microglial reaction to implantation of microelectrode through extension of processes. *Neural Eng.* 2012 **9** 066001. PMID 23075490

Lavinsky D, Sramek C, Wang J, Huie P, Dalal R, Mandel Y, Palanker D. 2014 Subvisible retinal laser therapy titration algorithm and tissue response. *Retina.* **34** 87-97. PubMed PMID 23873164.

Lee JE, Liang KJ, Fariss RN, Wong WT. 2008 Ex vivo dynamic imaging of retinal microglia using time-lapse confocal microscopy. *Invest Ophthalmol Vis Sci.*; **49** 4169–4176.

Majdi JA, Minnikanti S, Peixoto N, Agrawal A, Cohen ED. 2015 Access resistance of stimulation electrodes as a function of electrode proximity to the retina. *J Neural Eng.* **12** 016006.. PubMed PMID 25474329.

1 McCreery D B, Agnew W F, Yuen T G and Bullara L 1990 Charge density and charge per phase as
2 cofactors in neural injury induced by electrical stimulation *IEEE Trans. Biomed. Eng.* **37** 996–
3 1001
4

5
6
7 McLaren JW, Bourne WM, Patel SV. 2010 Standardization of corneal haze measurement in
8 confocal microscopy. *Invest Ophthalmol Vis Sci.* **51** 5610-6. PubMed PMID 20539002.
9

10
11
12 Minnikanti S, Cohen E and Peixoto N J 2010 Quasi-static analysis of electric field distributions by
13 disc electrodes in a rabbit eye model *Int. Fed. Med. Biol. Eng. Proc.* **32** 385–86
14
15

16
17
18 Nakauchi K, Fujikado T, Kanda H, Kusaka S, Ozawa M, Sakaguchi H, Ikuno Y, Kamei M and Tano Y
19 2007 Threshold suprachoroidal-transretinal stimulation current resulting in retinal damage in
20 rabbits *J. Neural. Eng.* **4** S50–7
21
22

23
24
25 Newman EA. 2001 Propagation of intercellular calcium waves in retinal astrocytes and Müller
26 cells. *J Neurosci.* **21** 2215-23. PubMed PMID 11264297;
27
28

29
30
31 Nimmerjahn A, Kirchhoff F and Helmchen F. 2005 Resting microglial cells are highly dynamic
32 surveillants of brain parenchyma in vivo *Science* **308** 1314-8.
33
34

35
36
37 O'Neill RJ, Tung L. 1991 Cell-attached patch clamp study of the electropermeabilization of
38 amphibian cardiac cells. *Biophys J.* **9** 1028-39. PubMed PMID 1907865
39
40

41
42
43 Opie NL, Greferath U, Vessey KA, Burkitt AN, Meffin H, Grayden DB, Fletcher EL. 2012 Retinal
44 prosthesis safety alterations in microglia morphology due to thermal damage and retinal
45 implant contact. *Invest Ophthalmol Vis Sci.* **53** 7802-12. PubMed PMID 23111605.
46
47

48
49
50 Paques M, Simonutti M, Augustin S, Goupille O, El Mathari B, Sahel JA. 2010 In vivo observation
51 of the locomotion of microglial cells in the retina. *Glia.* **58** 1663-8 PubMed PMID 20578032
52
53
54
55
56
57
58
59
60

1 Schindelin, J., Arganda-Carreras, I. and Frise, E. *et al.* 2012 "Fiji an open-source platform for
2 biological-image analysis", *Nature Methods*, **9** 676-682, PMID 22743772
3
4

5 Schmued LC, Hopkins KJ. 2000 Fluoro-Jade B a high affinity fluorescent marker for the
6 localization of neuronal degeneration. *Brain Res.* **874** 123-30. PubMed PMID 10960596.
7
8
9

10
11 Sim DA, Chu CJ, Selvam S, Powner MB, Liyanage S, Copland DA, Keane PA, Tufail A, Egan CA,
12 Bainbridge JW, Lee RW, Dick AD, Fruttiger M. 2015 A simple method for in vivo labelling of
13 infiltrating leukocytes in the mouse retina using indocyanine green dye. *Dis Model Mech.* **8**
14 1479-87. PMID 26398933
15
16
17
18

19
20 Tinevez JY, Perry N, Schindelin J, Hoopes GM, Reynolds GD, Laplantine E, Bednarek SY, Shorte
21 SL, Eliceiri KW. TrackMate 2017 An open and extensible platform for single-particle tracking.
22 *Methods.* **115** 80-90. PMID 27713081.
23
24
25
26

27 Uckermann O, Iandiev I, Francke M, Franze K, Grosche J, Wolf S, Kohen L, Wiedemann P,
28 Reichenbach A, Bringmann A. 2004 Selective staining by vital dyes of Müller glial cells in retinal
29 wholemounts. *Glia.* **45** 59-66. PubMed PMID 14648546.
30
31
32
33

34
35 Vrabec F. 1970 Microglia in the monkey and rabbit retina. *J Neuropathol Exp Neurol.* **29** 217-24.
36 PubMed PMID 4190979
37
38
39

40 Wen R, Song Y, Cheng T, Matthes M T, Yasumura D, LaVail M M and Steinberg R H 1995 Injury-
41 induced upregulation of bFGF and CNTF mRNAs in the rat retina *J. Neurosci.* **15** 7377–85
42
43
44

45
46 Wiley J D and Webster J G 1982 Analysis and control of the current distribution under circular
47 dispersive electrodes *IEEE Trans. Biomed. Eng.* **29** 381–5
48
49
50

51 Xia J, Lim JC, Lu W, Beckel JM, Macarak EJ, Laties AM, Mitchell CH. 2012 Neurons respond
52 directly to mechanical deformation with pannexin-mediated ATP release and autostimulation of
53 P2X7 receptors. *J Physiol.* **590** 2285-304.
54
55
56
57
58
59
60

1
2 Yue L, Falabella P, Christopher P, Wuyyuru V, Dorn J, Schor P, Greenberg RJ, Weiland JD,
3
4 Humayun MS. 2015 Ten-Year Follow-up of a Blind Patient Chronically Implanted with Epiretinal
5
6 Prosthesis Argus I. Ophthalmology. **122** 2545-52.e1. PubMed PMID 26386850
7
8
9
10
11
12
13
14
15
16
17
18
19
20
21
22
23
24
25
26
27
28
29
30
31
32
33
34
35
36
37
38
39
40
41
42
43
44
45
46
47
48
49
50
51
52
53
54
55
56
57
58
59
60

Figures

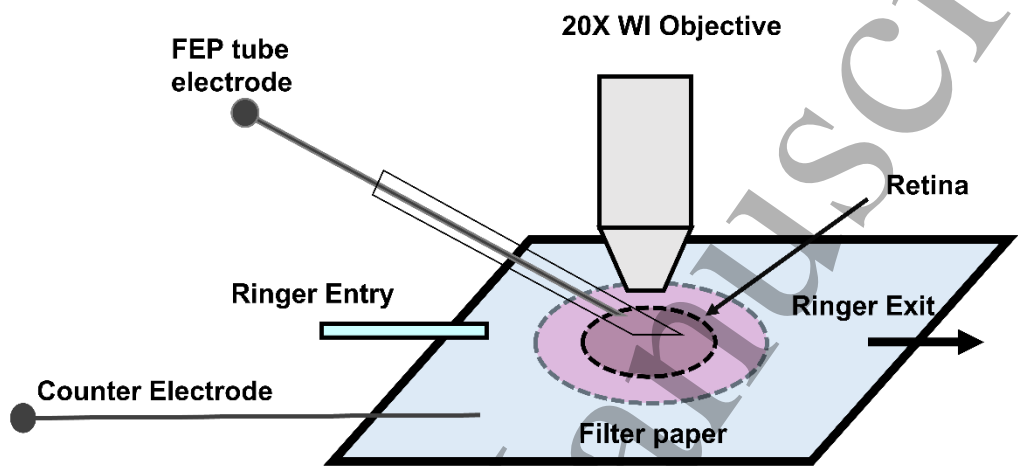


Figure 1. Setup for real-time confocal imaging of the microglia under a stimulus electrode. The isolated retina was mounted on filter paper (dashed line) and superfused with an oxygenated Ringer solution. To electrically stimulate the retina (dashed), a thin-walled optically transparent saline-filled fluoropolymer stimulation electrode tube was positioned under the water immersion microscope objective to efface flat against the inner retinal surface. The confocal microscope optically sectioned through the retina underneath the tube during the electrical pulse stimulation experiment. Current pulses passed across the retinal layers to a broad counter electrode located in the side of the recording chamber bath.

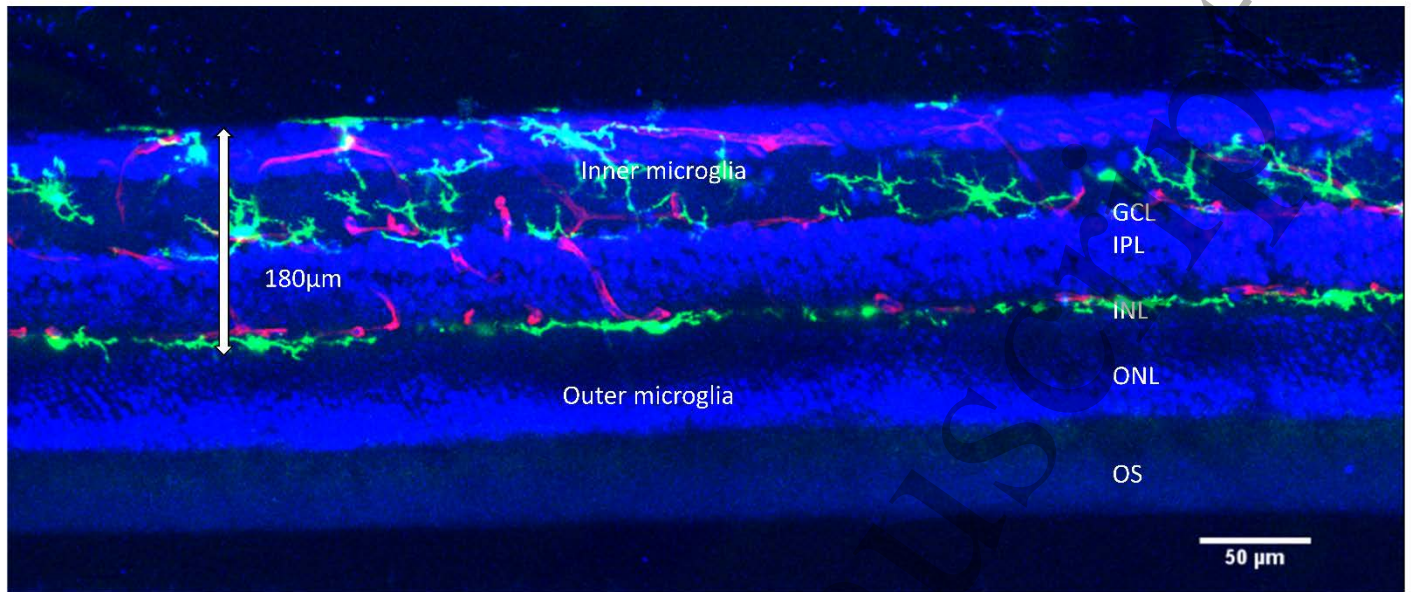


Figure 2 Confocal microscope image of the microglia distribution in a retinal slice from the CX3CR1 fractalkine mouse. In this mouse retina, the GFP labeled microglia are fluorescent and distributed in 2 bands, similar to humans. The inner microglia band is broad and extends from superficial microglia at the inner limiting membrane (ILM) and ganglion cell layer (GCL) to microglia arborizing in the inner plexiform layer (IPL). The outer microglia band is narrow in normals and consists of highly branched microglia with planar arborizations in the outer plexiform layer (OPL). The white arrow shows the approximate extent of the retina imaged under the transparent stimulation electrode. Red fluorescence denotes blood vessels labeled with tomato lectin, while blue denotes nuclei stained with DAPI. INL, Inner nuclear layer, ONL, Outer nuclear layer, OS Outer segments of photoreceptors.

1
2
3
4
5
6
7
8
9
10
11
12
13
14
15
16
17
18
19
20
21
22
23
24
25
26
27
28
29
30
31
32
33
34
35
36
37
38
39
40
41
42
43
44
45
46
47
48
49
50
51
52
53
54
55
56
57
58
59
60

Accepted Manuscript

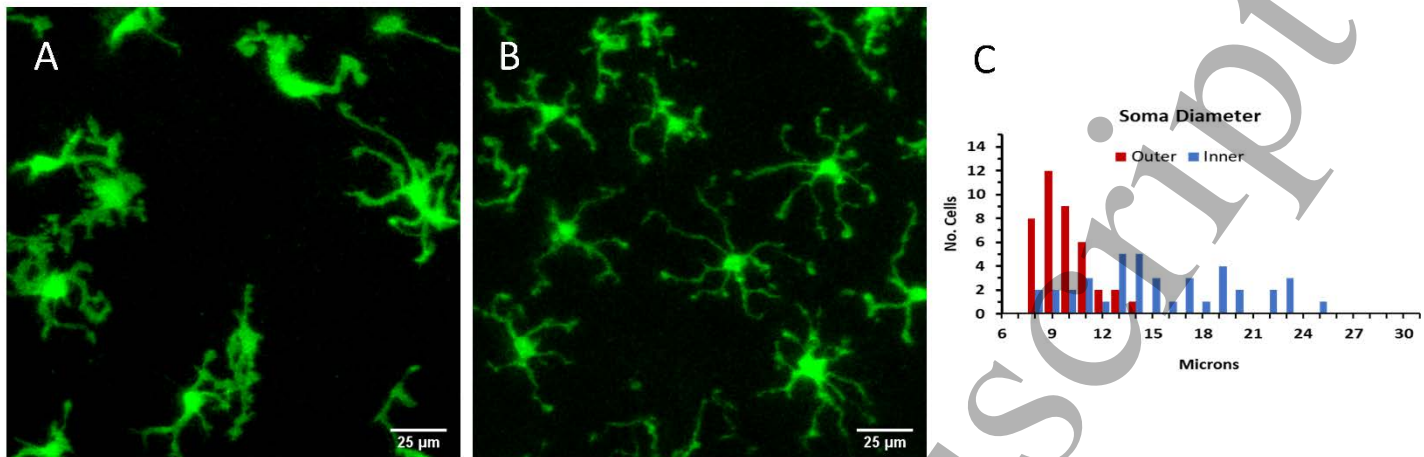


Figure 3. Confocal microscope image stack of the same retinal microglia field at 2 substack focal planes. A. Inner retinal microglia have large cell bodies and variable processes. B. Outer retinal microglia have smaller cell bodies and tend to be finely branching. C. Frequency histogram of the distribution of the soma diameters of 40 inner and outer microglia measured from the same image stack field from 4 retinas. Soma diameter was derived from areal measurements using confocal microscope z-substacks of the inner or outer microglia (See Methods for details).

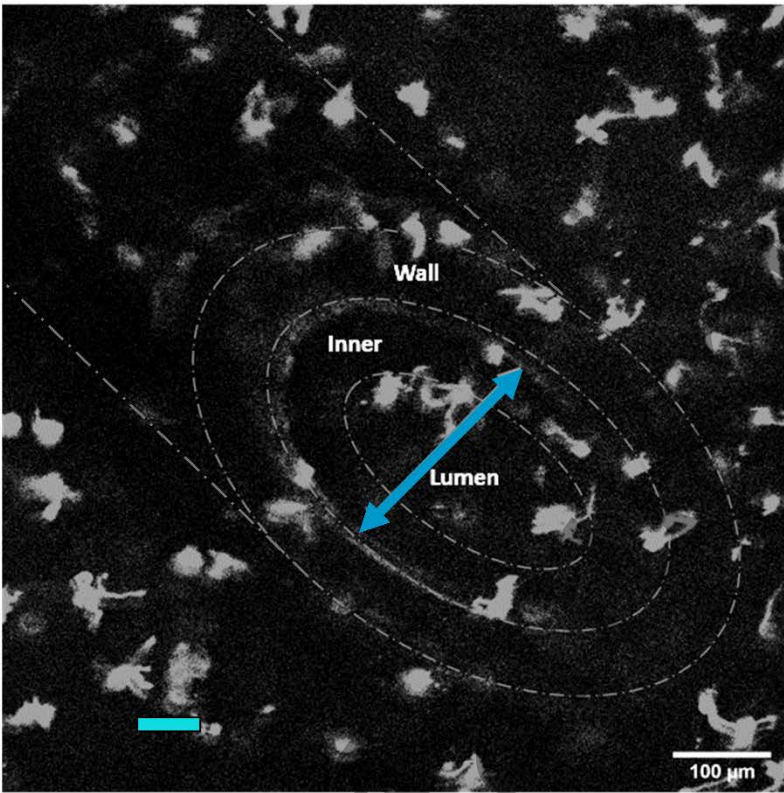


Figure 4. Zones of microglia analysis and confocal imaging time line for an electrical overstimulation experiment with a transparent electrode. The fluopolymer stimulation tube (dashed lines) enters the image at the top left corner and its lumen was placed against the retinal surface. The electrode lumen edges are dimly visible in this contrast-enhanced confocal image, its width shown by the arrow, and the three zones of microglial analysis are indicated by dashed concentric ellipses. The time line of imaging confocal z-stacks every 2.5 min is shown at bottom. After the 10 min. period of baseline images, a 5 min. period of overstimulation pulses occurred (blue bar), followed by a 60min period of recovery, and then labeling for cellular damage with the nuclear dye 7AAD.

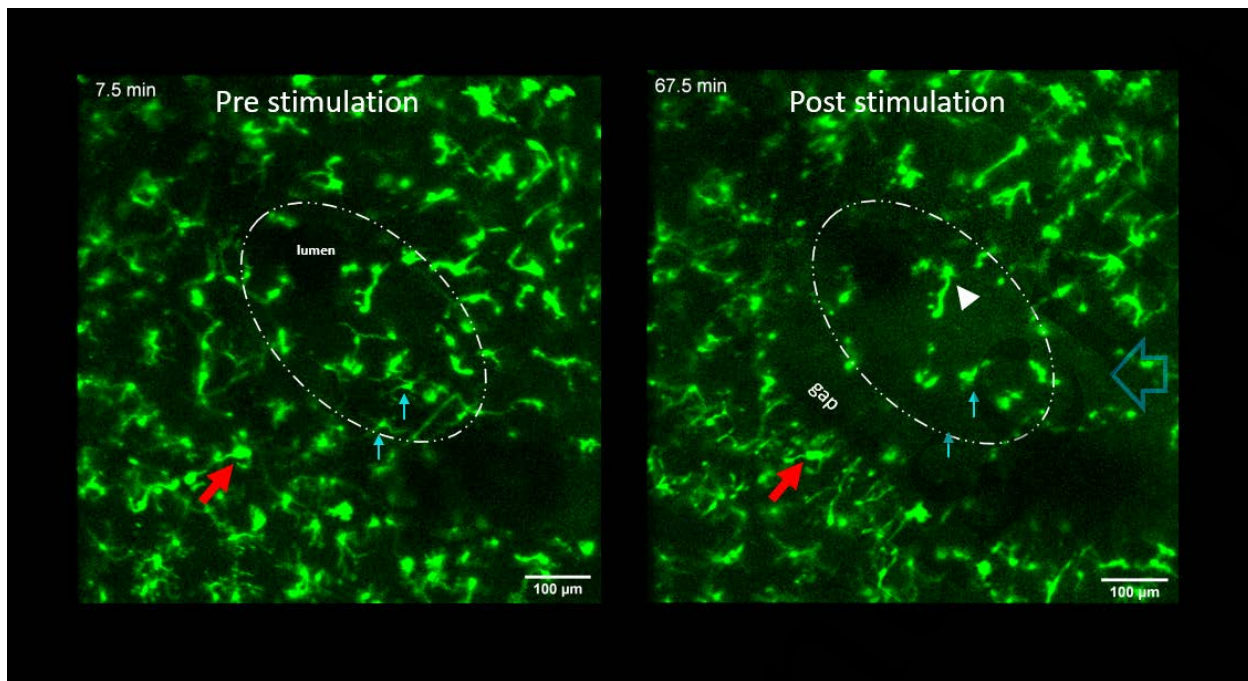


Figure 5. Time lapse confocal microscope Z-stack images of the field of fluorescent microglia under an optically transparent stimulus electrode before and after $749\mu\text{C}/\text{cm}^2/\text{ph}$ overstimulation. The position of the electrode lumen is shown by the dashed white line. Left Confocal Z-stack image of the microglial distribution pre stimulation. Both large (red arrow) and small soma (blue arrows) microglia are present around the electrode and their filopodia are randomly oriented. Right Effect of electrical overstimulation on the retinal microglia 52.5 min post stimulation. A 5 min. train of biphasic pulses was applied at $t=10\text{min}$. After the pulses, a circular zone of hypofluorescence (gap) developed around the electrode wall. In the electrode lumen, the larger soma microglia appear heavily blebbed and immotile, with a single weak survivor (arrowhead), and the image of the small soma microglia began to disappear (small blue arrows). Around the electrode edge, the larger soma microglia respond to the injury by extending and orienting filopodia inward. Large arrow denotes Ringer flow direction. (See Z-stack image Movie 2).

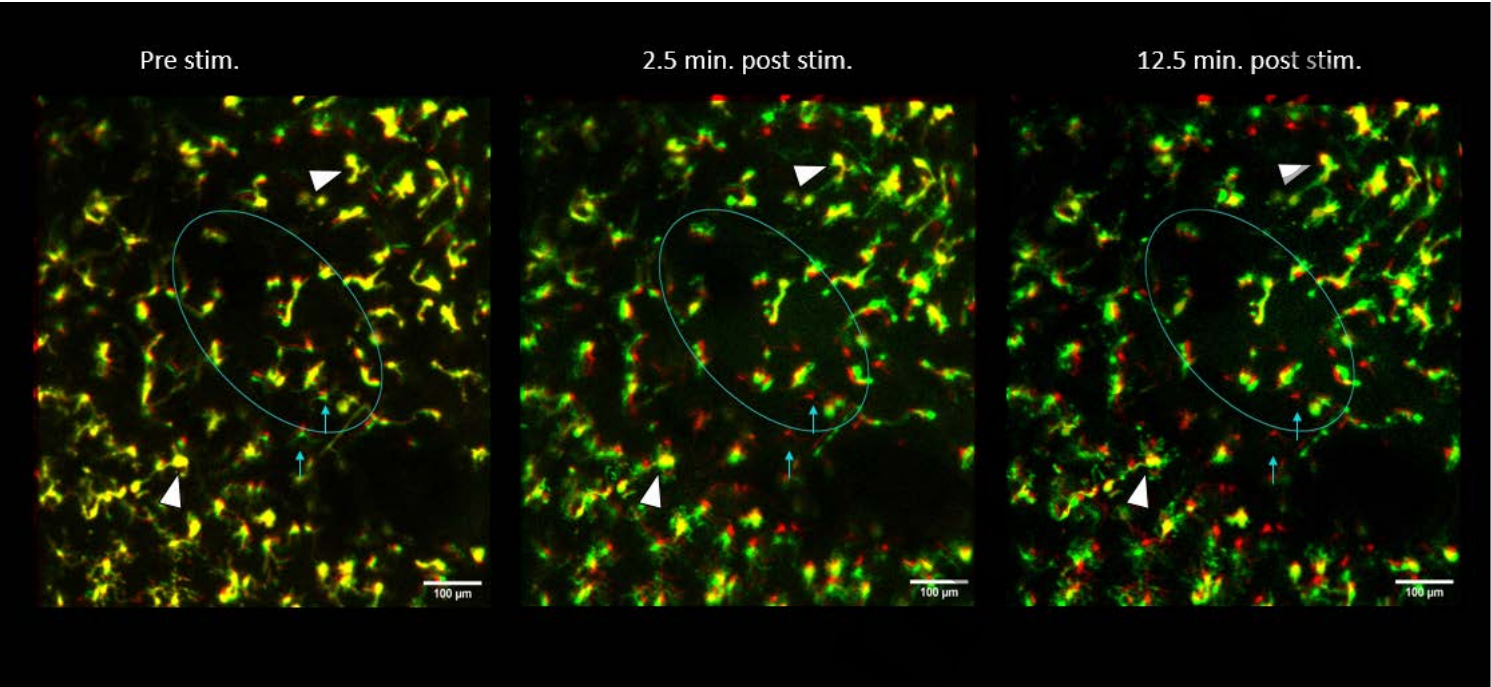


Fig. 6. Comparison of the temporal changes in the microglia field morphology under the transparent stimulus electrode at different times before and after the overstimulation. In each panel the microglial field just prior to stimulation is shown in red ($t=7.5\text{min}$), while the comparison field at different time points is shown superimposed in green. Left panel: Comparison of unstimulated microglia at start of image session ($t=0\text{min}$) to $t=7.5$, shows only minor changes in processes morphology and overlapped cells are yellow. Middle panel: In contrast, 2.5 minutes after overstimulation, many microglia change their morphology with green process growth (arrowheads), while a few microglia in the far periphery remain unchanged. Right panel: At 12.5 minutes post stimulation, many microglia around the electrode grow green processes which are oriented toward the damage zone. The few cells that remain unchanged appear yellow. Blue arrows show small microglia, which disappear after stimulation (see text for details). Lumen shown as before.

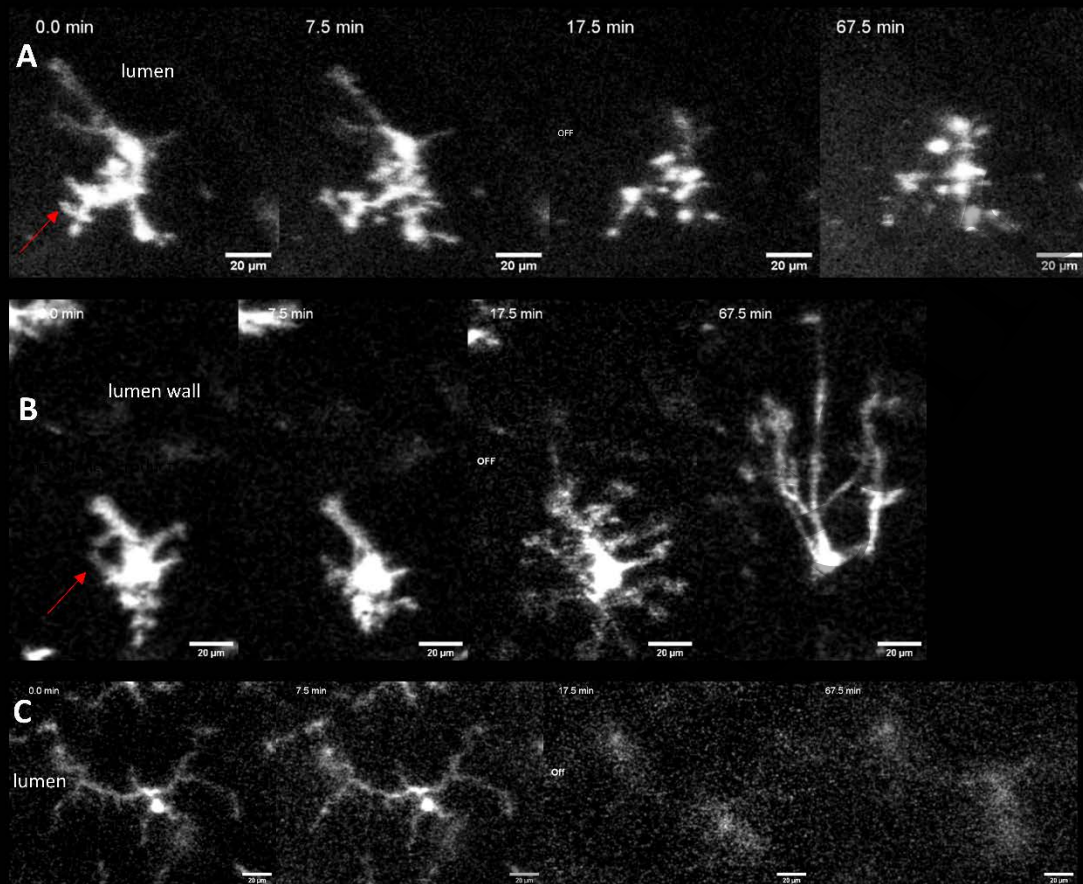


Fig 7. Time-lapse confocal images from 749uC/cm²/ph overstimulation movies showing the three microglia response pattern morphologies seen and their imaged locations. The GFP labeled microglia filopodia (arrows) are shown in 4 time-series panels pre (0, 7.5 min.), and post stimulation (17.5 (2.5min post), 67.5 min (52.5min post)). A. Inside electrode lumen. Example of an “immotile” microglia morphology resulting from overstimulation. The microglia soma has shrunk and only a series of ball-like appendages remain suggesting severe injury/death. The fluorescence of the cell declined. B. Outside electrode wall. Example of a “responder” microglia changing shape rapidly post stimulation; extending processes into the inner damage zone under the electrode wall. The filopodia of the responder cells were highly motile post-stimulation, their central soma was well defined, and their fluorescence remained. C. Inside electrode lumen. Example of a “fading” microglia under the electrode whose general fluorescent image signal became blurred post stimulation, which may be due to increased optical scatter in the image from proximal tissue swelling after overstimulation. For time-lapse movies of each figure, see supplemental data (See image movies 3, 4, and 5).

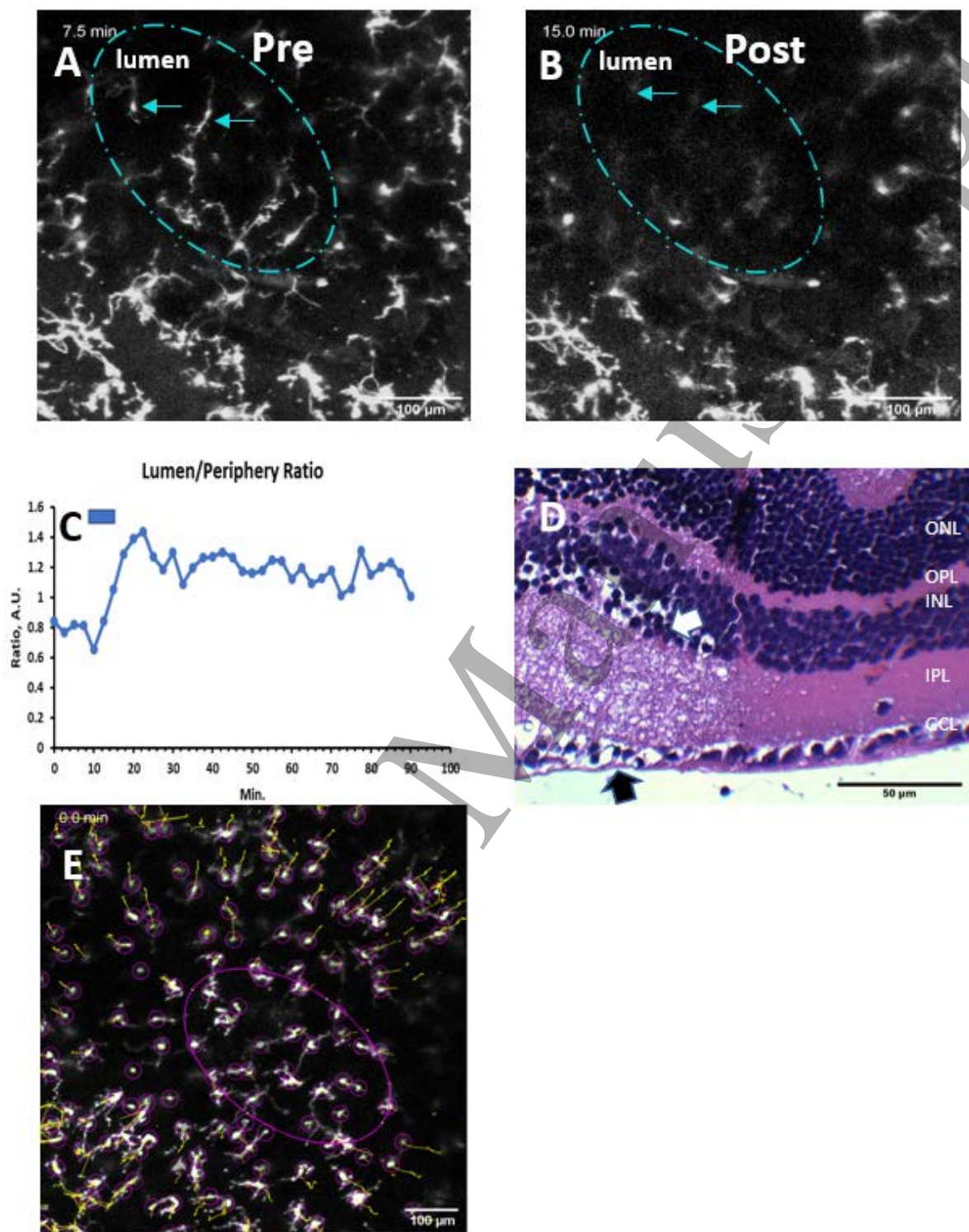


Figure 8. Retinal swelling under the electrode after 749uC/cm2/ph electrical stimulation pulses causes increased optical scatter in outer microglia confocal images. A.B. Time-lapse confocal microscopic Z-substacks selectively imaging the outer microglia layer in the OPL pre and post stimulation. In the prestimulus condition (Pre), the small microglia in the lumen (dashed line) are visible. Immediately after the pulsing (Post), their fluorescent morphology

1 is blurred by an increase in tissue scatter in the optical path identifying them as “fading” cells.
2 C. Graph showing the scatter ratio in z-stack images between zones in the lumen and the
3 periphery before and after stimulation. After pulsing (bar), a rapid increase in scatter ratio
4 starts which persists for the imaging period. D. Histological comparison of a stimulated retinal
5 zone next to neighboring retinal tissue. In the stimulation zone, swelling is seen in the
6 ganglion cell layer (black arrow), the inner plexiform layer, and the lower inner nuclear layer
7 (white arrow). However, there is less damage in the OPL. E. Time-lapse position tracks
8 (yellow) of outer retinal microglia somata Z-substacks around the electrode are displaced
9 centrifugally by overstimulation, as shown superimposed on the first image. Microglia under
10 the lumen area (purple line) faded and could not be tracked. IPL inner plexiform layer, ONL,
11 outer nuclear layer, OPL, outer plexiform layer, INL, Inner nuclear layer, GCL, ganglion cell
12 layer
13
14
15
16
17
18
19
20
21
22
23
24
25
26
27
28
29
30
31
32
33
34
35
36
37
38
39
40
41
42
43
44
45
46
47
48
49
50
51
52
53
54
55
56
57
58
59
60

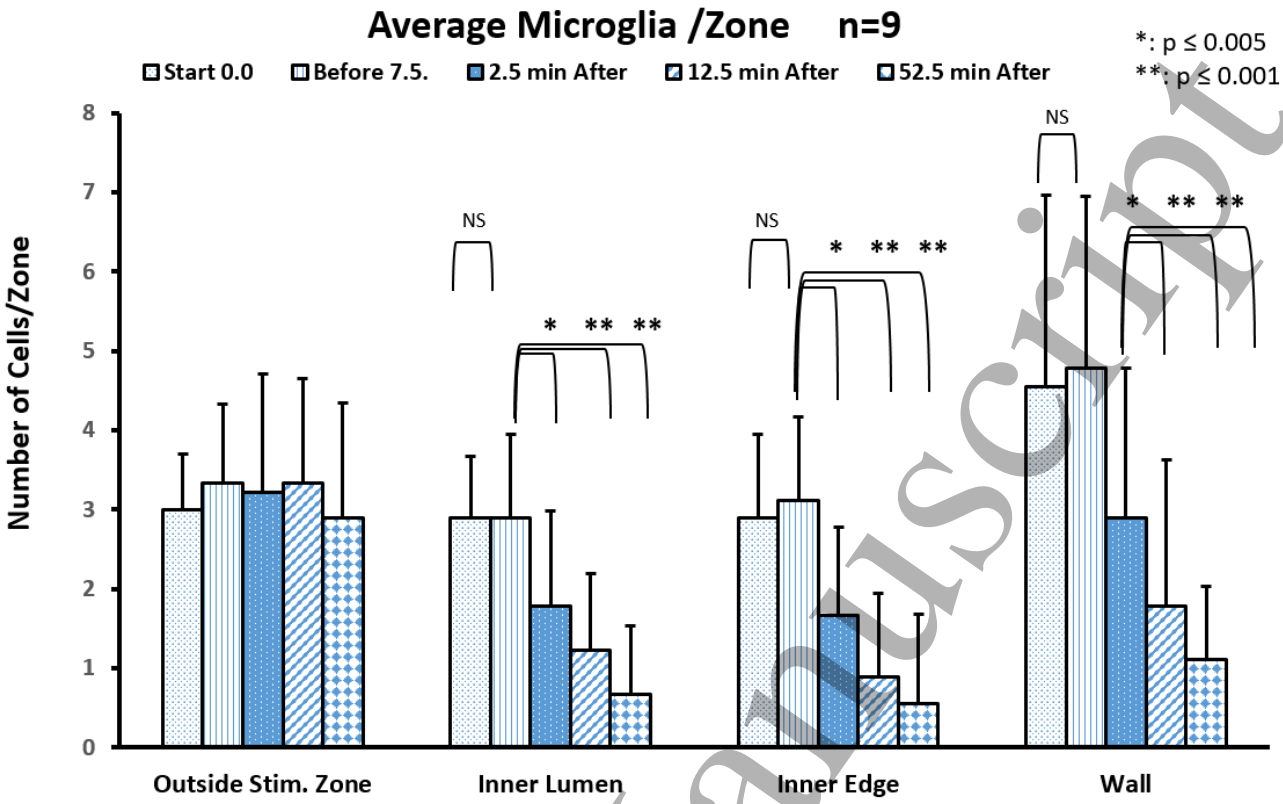


Figure 9 Effect of electrical overstimulation at 749uC/cm2/ph on the average number of live large microglia in the 3 analysis zones under the transparent stimulation electrode. Bars denote number of live microglia seen before (0, 7.5 min), and 2.5, 12.5 and 52.5 minutes post stimulation. Microglia that were immotile/or lost fluorescence were scored as dead. The largest loss of cells occurred at the first analysis period post stimulation (2.5 min after/ 42%), but cell loss continued even to the end of the imaging period. Error bars denote standard deviation. The microglia with small cell bodies in the outer plexiform layer were not analyzed in this assessment.

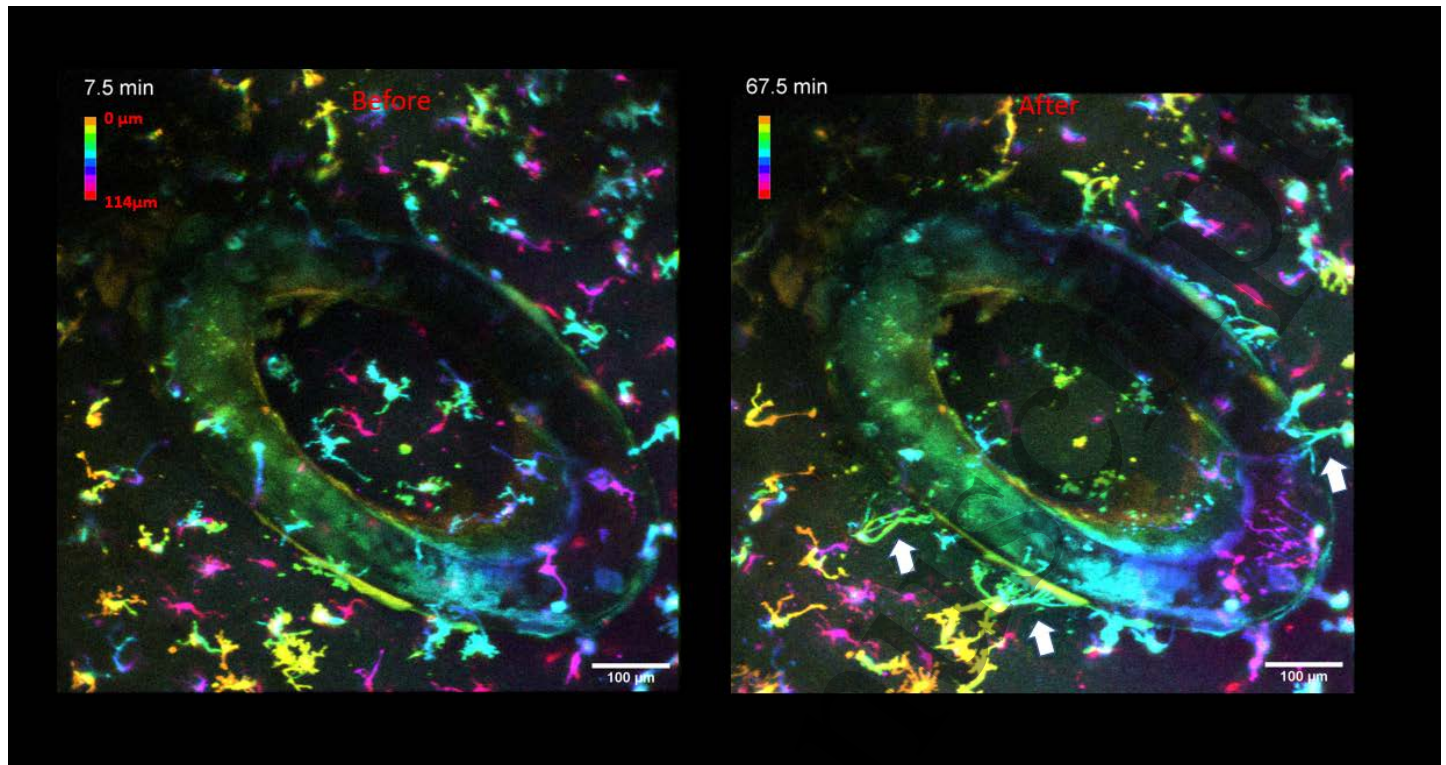


Figure 10. Identification of the microglia layers responding to 749uC/cm²/ph overstimulation using color encoded depth Z-stack movie images. The panels show the microglia morphology in the retina before and after overstimulation under the transparent electrode. In this depth encoded movie, microglia near the inner limiting membrane/IPL are colored yellow-cyan, while the deeper microglia farther from the electrode in the outer plexiform layer are colored red-pink. The main morphological “responders” to overstimulation tended to be the inner retinal microglia. Left panel Z-stack just before stimulation. Right panel Z-stack 52.5 minutes post stimulation. After stimulation, inner microglia inside the electrode lumen and wall are largely immotile and increased scatter in the lumen is present. Externally many inner retinal microglia extend filopodia around and over the stimulation electrode wall (white arrows). Depth scale color bar denotes cell level in confocal image stack of 114μm with position 0um being at the inner retinal surface near the electrode. See supplemental data for full time-lapse movie. The electrode edges are enhanced slightly by the contrast algorithms used to reconstruct the microglia field.

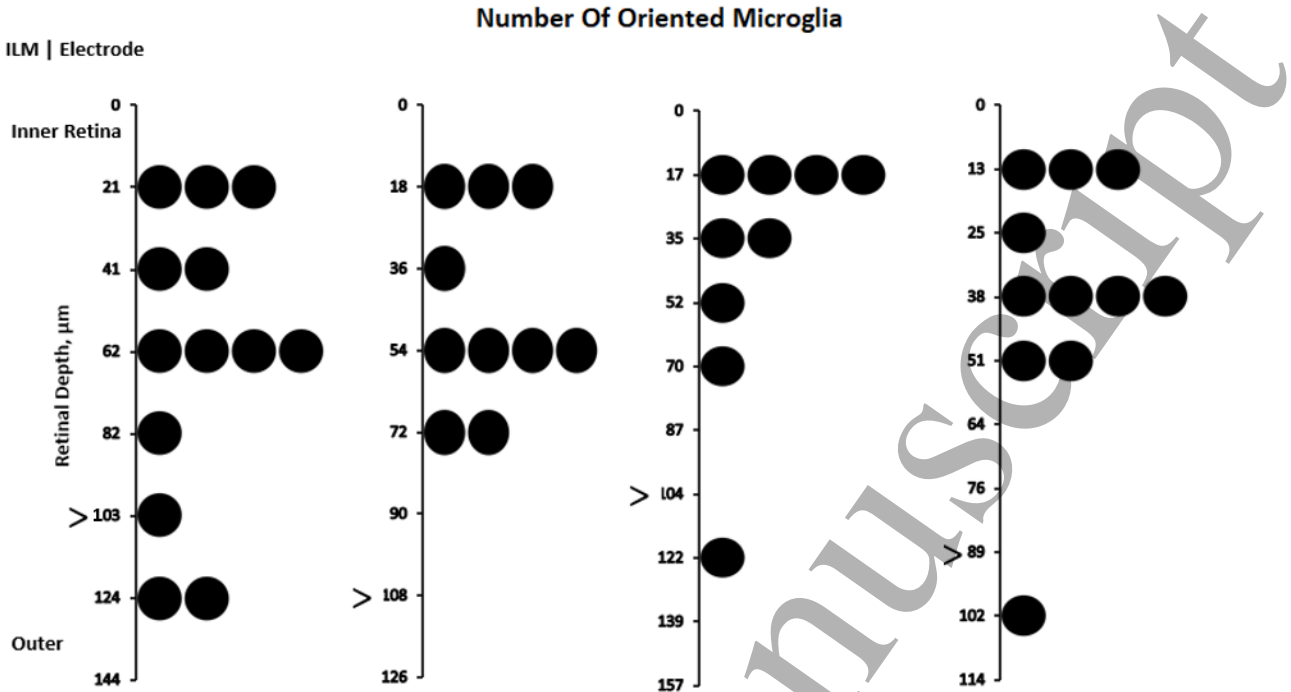


Figure 11. Dot plot charts show the “responder” microglia population after overstimulation was mainly composed of cells from the inner retina. Each dot shows the retinal depth location of the soma of a responder microglia outside the tube with directional filopodia growth towards the electrode wall from the confocal image stacks. Microglia with directional filopodia were identified at the 52.5 minutes post pulse stimulation and tracked in reverse to get their pre stimulus period soma positions. The soma position level is shown for microglia before stimulation (7.5min), where each dot shows the retinal depth of individual microglia located $\leq 120\mu\text{m}$ laterally from the outer electrode wall. Dots at or below the “>” marker denote microglia somas located in the OPL for each image series stack.

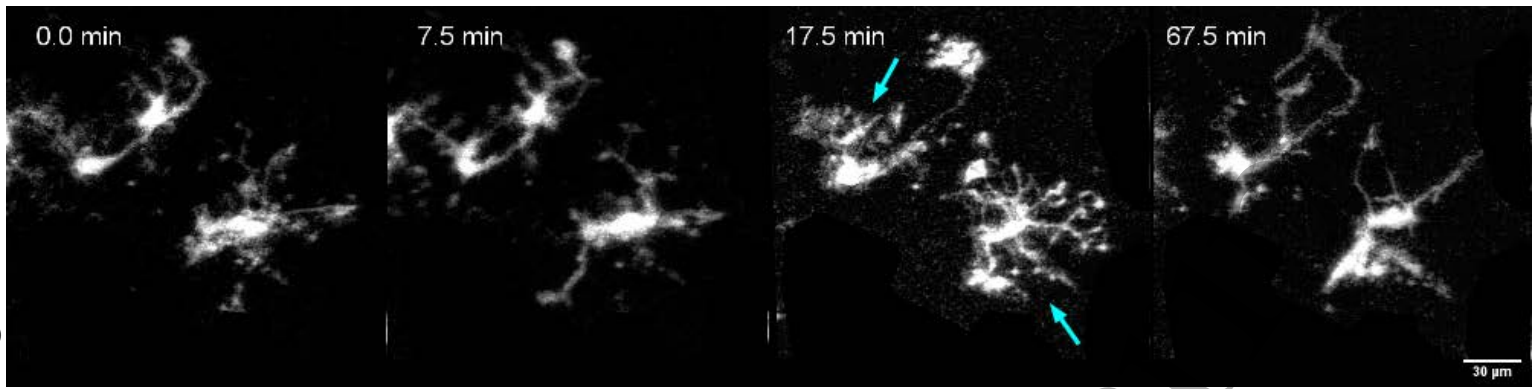


Figure 12. Time-lapse confocal images movies showing 2 microglia inside the electrode lumen responding to $442\mu\text{C}/\text{cm}^2/\text{ph}$, a lower level of overstimulation (inner edge zone). The GFP labeled microglia filopodia are shown in 4 time-series panels: pre- (0, 7.5 min.), and post-stimulation (17.5 (2.5min post), and 67.5 min (52.5min post)). Stimulation at $442\mu\text{C}/\text{cm}^2/\text{ph}$ often caused significant process outgrowth post stimulation (blue arrows, responder morphology) followed by retraction during the recovery interval. The outer microglia have been removed from the time-lapse montage images for clarity.

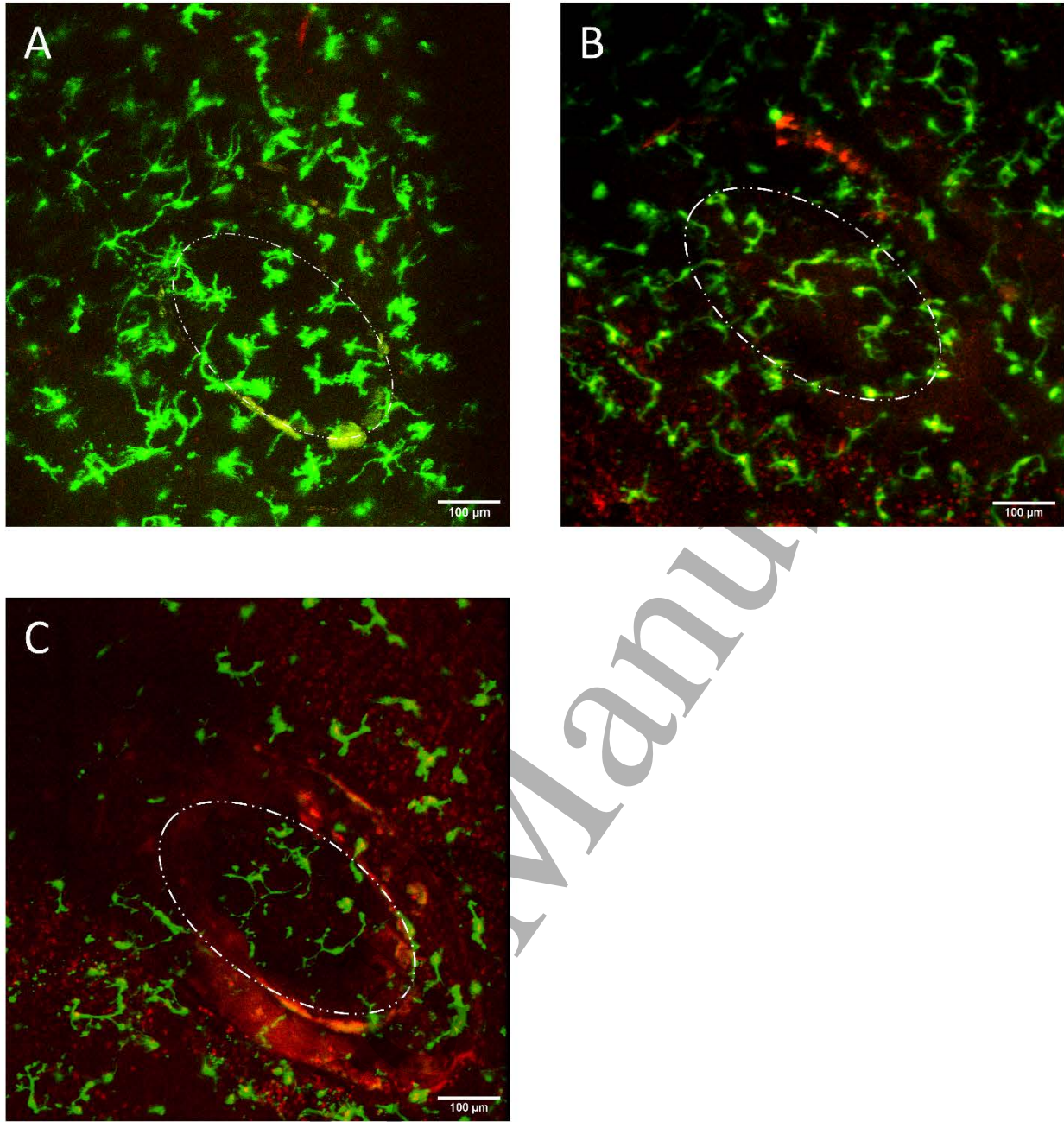


Figure 13. Comparison of 7AAD stain for injury with EGFP microglia fluorescence stacks at 3 stimulation levels. A. Control, unstimulated retina, 60 mins post stimulation. The microglia are not oriented and there is little damage. There is little staining with the nuclear dye 7AAD. B. Post stimulation 442 μ C/cm²/ph. Some 7AAD stain is present. C. Post stimulation 749 μ C/cm²/ph. There are contracted microglia, extensive 7AAD stain around the electrode, and in the lumen.

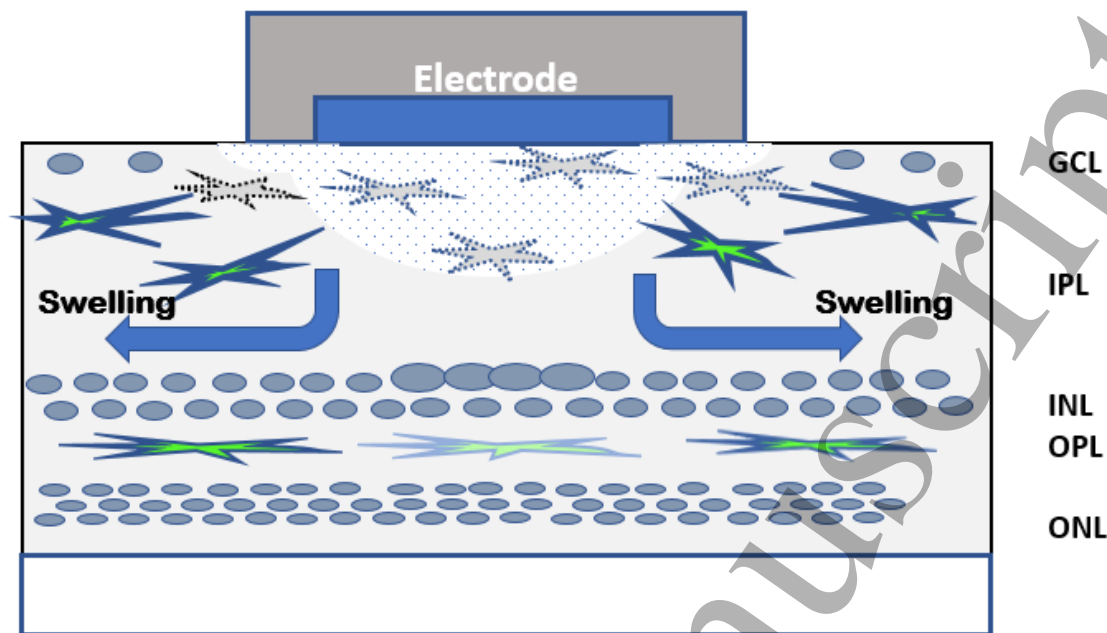


Figure 14. Model accounting for the effects of overstimulation on the retinal microglia experimentally seen under transparent epiretinal stimulus electrodes. Overstimulation of the retinal tissue by the E-field (dotted) directly under the electrode causes edema, optical scatter, and lateral displacement of the neuropil due to electrode confinement. The microglia and inner cells are injured directly under the electrode (grey), while the healthy microglia outside the stimulus electrode walls (green) “respond” to the injury with oriented filopodia growth and become activated. Due to fluorescence scatter through the overlying edematous retina, the fluorescent confocal image of outer retinal microglia appear to “fade” underneath the electrode.